

On the role of eigenvalue disparity and coordinate transformations in the reduction of the linear noise approximation

Justin Eilertsen^a, Wylie Stroberg^b

^a*Mathematical Reviews, American Mathematical Society, 416 4th Street, Ann Arbor, MI 48103, USA*

e-mail: jse@ams.org

^b*Department of Mechanical Engineering, University of Alberta, Edmonton, Alberta, Canada*

email: stroberg@ualberta.ca

Abstract

Eigenvalue disparity, also known as timescale separation, permits the systematic reduction of deterministic models of enzyme kinetics. Geometric singular perturbation theory, of which eigenvalue disparity is central, provides a coordinate-free framework for deriving reduced mass action models in the deterministic realm. Moreover, homologous deterministic reductions are often employed in stochastic models to reduce the computational complexity required to simulate reactions with the Gillespie algorithm. Interestingly, several detailed studies indicate that timescale separation does not always guarantee the accuracy of reduced stochastic models. In this work, we examine the roles of timescale separation and coordinate transformations in the reduction of the Linear Noise Approximation (LNA) and, unlike previous studies, we do not require the system to be comprised of distinct fast and slow variables. Instead, we adopt a coordinate-free approach. We demonstrate that eigenvalue disparity does not guarantee the accuracy of the reduced LNA, known as the slow scale LNA (ssLNA). However, the inaccuracy of the ssLNA can often be eliminated with a proper coordinate transformation. For planar systems in separated (standard) form, we prove that the error between the variances of the slow variable generated by the LNA and the ssLNA is $\mathcal{O}(\varepsilon)$, where ε is a dimensionless number proportional to the eigenvalue ratio. We also address a case in which all eigenvalues vanish in an appropriate singular limit, resulting in a nilpotent Jacobian that signals the breakdown of classical singular perturbation theory. We use the blow-up method to construct a reduced equation that is accurate near the singular limit in the deterministic regime. However, this reduction in the stochastic regime is far less accurate, which illustrates that eigenvalue disparity plays a central role in stochastic model reduction.

Keywords: Singular perturbation, stochastic process, quasi-steady-state approximation, Michaelis–Menten reaction mechanism, Langevin equation, linear noise approximation, slow scale linear noise approximation

1. Introduction

The derivation of accurate, low-dimensional reduced models of chemical reactions is a coveted element of mathematical and computational biology. Low-dimensional deterministic ordinary differential equation (ODE) models of biochemical reactions play a critical

role in drug design and drug targeting: kinetic parameters are estimated by fitting experimental timecourse data to reduced ODE models such as the standard Michaelis-Menten rate law [1]. In addition, the reduction of stochastic models permits a favorable trade-off between accuracy and computational complexity: a high-dimensional stochastic model of a biochemical reaction can often be replaced with a low-dimensional model with a negligible cost in accuracy and a substantial reduction in computational complexity [2, 3].

The mathematical feature responsible for the permission of model reduction is *timescale separation*. Chemically, if a reaction mechanism is comprised of several elementary reactions, timescale separation implies that the corresponding rates of the elementary reactions are disparate: some reactions may unfold slowly or occur with less frequency than others. Mathematically, timescale separation implies that the Jacobian matrix of the linearized model has a significant spectral gap.

Reduction of deterministic ODE models is based on well-established theory; specifically, geometric singular perturbation theory (GSPT) [4, 5, 6, 7]. In short, reduced deterministic models are generated by (approximately) projecting vector fields on \mathbb{R}^n onto the s -dimensional tangent space ($s < n$) of an attracting and invariant s -dimensional submanifold of \mathbb{R}^n (i.e., a slow manifold). The resulting *projected* ODE is a s -dimensional dynamical system that accurately describes the long-time behavior of the reaction mechanism it models. GSPT provides a coordinate-free framework for deriving reduced ODE models. This is particularly useful in applications where one is usually interested in working with physically meaningful variables.

The extension of GSPT to linear and nonlinear stochastic differential equations (SDEs) driven by a Wiener process is also fairly widespread [8]. However, the appropriate stochastic description of a reaction mechanism depends on the size of the chemical system: deterministic models prevail when the system size is large; stochastic models prevail when the system size is small [9]. The chemical master equation (CME) provides the fundamental description of chemical reaction kinetics, especially when the size of the system is small. Unfortunately, CMEs are difficult to analyze directly and, consequently, reduced CMEs are often generated by the heuristic application of deterministic reduction methodologies. Such a procedure generates a *heuristically reduced* CME (*hCME*). Incredibly, and perhaps somewhat surprisingly, *hCMEs* have been shown to be highly accurate [10, 3, 11, 12]. However, Janssen [13] demonstrated that the heuristic approach can fail, even though both the stochastic and deterministic models of the associated reaction mechanism exhibit timescale disparity. Several additional studies arrived at the same conclusion: timescale separation does not guarantee that the *hCME* is accurate [14, 15, 16]. This begs the question: Why is the presence of noise sometimes an obstacle in stochastic model reduction?

The objective of this paper is to gain a mathematical understanding of why *hCMEs* fail despite the presence of timescale disparity. To circumvent the difficulty of working with the CME directly, we appeal to the linear noise approximation (LNA). The LNA is valid near the thermodynamic limit when the system size is extremely large but not large enough to suppress intrinsic noise. In the LNA regime, the temporal dynamics of the mean-field concentrations of the chemical species that comprise a reaction network satisfy the deterministic mass action equations; random departures from the mean-field approximation are described by an Ornstein-Uhlenbeck process, defined by a linear stochastic differential equation (SDE); see FIG. 1 for a qualitative illustration.

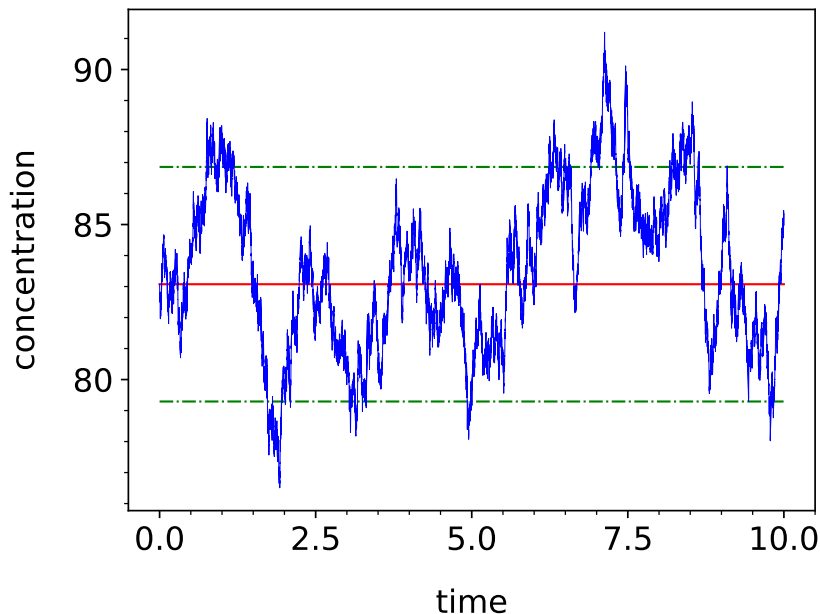


Figure 1: **The concentrations of chemical species randomly fluctuate around the mean-field approximation in the LNA regime.** In this figure, the mean-field concentration under steady-state conditions is demarcated by the horizontal red line. The blue line is the concentration given by the LNA that includes the random fluctuations around the mean-field (steady-state) concentration. The green lines are the mean-field approximation \pm one standard deviation. Our interest in this work is the ability of various reduced LNAs to accurately approximate the standard deviation of the LNA under steady-state conditions. The units of concentration and time are arbitrary. This figure was generated by numerically solving the LNA (67) with parameters (in arbitrary units): $s_0 = 100, k_1 = 2.0, k_{-1} = 20.0 = k_2, e_0 = 1.0, k_3 = 1.0$.

To enhance the understanding of stochastic model reduction in chemical kinetics and shed light on the occasional failure of h CMEs, we will focus on the reduction of the LNA. Since h CMEs admit a heuristic LNA (h LNA), understanding the failure of the h LNA will help to explain why h CMEs also fail¹. In particular, we will analyze the ability of the slow scale LNA (ssLNA) to accurately approximate the variance of the fluctuations about the mean-field approximation. We show that the ssLNA is actually the projection of the LNA onto the slow eigenspace defined by the Jacobian of the mean-field (mass action) equations evaluated at the steady-state concentration. Our definition of ssLNA is more general than previous definitions [14, 18, 19] and does not require the underlying deterministic system to be expressed in terms of distinct fast and slow variables. Furthermore, we introduce the *fast scale* LNA (fs LNA), which is the approximate projection of the LNA onto the corresponding fast eigenspace.²

¹The idea to compare h LNAs to ssLNAs was first conceived by Thomas et al. [17].

²Fast dynamics were approximated in [18] over the complete timecourse of the reaction but not in a coordinate-free context: the underlying deterministic system was assumed to have distinct fast and slow variables.

Although principal to singular perturbation theory, the concept of timescale separation is somewhat vague in previous studies [14, 18, 19, 10]. This is primarily because highly cited deterministic analyses rely on non-dimensionalization, scaling, and heuristics such as nonlinear timescales [20, 21], and the techniques employed in these works carried over to the stochastic worldview. Unless extreme care is taken, scaling and non-dimensionalization can lead to scenarios where singular perturbation theory does not hold or, perhaps more importantly, can generate erroneous conclusions concerning the type of singular perturbation and the labeling of fast and slow variables [22]. The recent development of Tikhonov-Fenichel Parameter Value theory is a powerful methodology that ensures the consistency of a deterministic reduction with a specific singular perturbation scenario but also avoids the a priori need to scale and non-dimensionalize the model equations [23, 24]. We use Tikhonov-Fenichel Parameter Value theory to avoid the potential pitfalls of scaling analysis. We also measure timescale separation by eigenvalue disparity and do not rely on “nonlinear” timescales.

In what follows, by considering both the *ssLNA* and *fsLNA*, we: (i) explain why timescale separation is not sufficient to ensure not only the accuracy of the *hLNA* but also, in some cases, the *ssLNA*; (ii) show that the accuracy of reduced LNAs can often be recovered with an appropriate coordinate transformation. In short, we demonstrate that, unlike the reduction of deterministic ODE models, the accuracy of reduced stochastic models is sensitive to the choice of coordinate system.

In addition, we re-analyze one of the original models introduced by Janssen [13]. The work by Janssen [13] is used as an example of why *hCMEs* should be employed with caution. In it, Janssen illustrated that the *hCME* can fail even when the underlying deterministic singularly perturbed problem has distinct fast and slow variables, but did not explain why the failure occurs. Interestingly, a discussion on eigenvalue disparity was notably absent from Janssen’s work. We show that the scenario explored by Janssen is void of appropriate eigenvalue disparity in the singular limit. Furthermore, the derivation of a reduced model in such situations is not problematic in deterministic regimes: the blow-up method (see Kuehn [25], Ch. 7 as well as [26] and Wechselberger [7], Ch.5 Section 5.3) can produce a highly accurate reduction that is valid near the singular limit. While the lack of eigenvalue disparity is not an obstacle in the reduction of deterministic models, we show that stochastic reduction based on the deterministic reduction is less reliable.

The paper is organized as follows: in Section 2 we will review the established results in deterministic and stochastic model reduction as it pertains to general dynamical systems and chemical kinetics. In Section 3 we introduce the *fsLNA* and demonstrate why timescale separation does not always ensure that certain reduced models are accurate. More importantly, we prove that the error between the variance of the slow variable obtained from the *LNA* and the variance of the slow variable obtained from the *ssLNA* is $\mathcal{O}(\varepsilon)$ when the variables are separated into distinct fast and slow coordinates (i.e., when the underlying singularly perturbed system is in standard form). Case studies of various chemical systems are presented in Section 4. In Section 5 we revisit the reduction of the *CME* and comment on the implications of the results presented in Section 3. In Section 6 we discuss the *open* Michaelis-Menten reaction mechanism and explain why the heuristic reduction fails, as reported by Thomas et al. [14]. We conclude with the re-analysis of Janssen’s work and a discussion of future work.

2. Deterministic and stochastic model reduction: A review of pertinent results

In this section we review the basic of singular perturbation theory as it applies to linear, deterministic equations. We also derive the ssLNA directly from singular perturbation theory. However, some remarks are in order. First, it necessary to distinguish between points in \mathbb{R}^n and vectors. Points (coordinates) in \mathbb{R}^n will generally be denoted as (z_1, z_2, \dots, z_n) , and vectors as $(z_1, z_2, \dots, z_n)^T$. By *manifold*, we mean a submanifold of \mathbb{R}^n , since \mathbb{R}^n is itself a manifold. For our purposes, it will suffice to define an s -dimensional submanifold of \mathbb{R}^n , S , as a collection of points in \mathbb{R}^n that comprise the regular level set of a function, $f : \mathbb{R}^n \mapsto \mathbb{R}^{n-s}$:

$$S := \{z \in \mathbb{R}^n : f(z) = 0\}, \quad \text{with rank } Df(z) = n - s \quad \forall z \in S. \quad (1)$$

The tangent space to S at a point $z \in S$ is denoted by $T_z S$, is an s -dimensional vector subspace of $T_z \mathbb{R}^n$, the tangent space of \mathbb{R}^n at z . Elements of $T_z \mathbb{R}^n$ are vectors, and are represented with vector notation. However, we will usually drop the notation $T_x \mathbb{R}^n$, and \mathbb{R}^n will be used to refer to the collection of points (n -tuples) of the form (z_1, z_2, \dots, z_n) as well as an n -dimensional vector space with elements $(z_1, z_2, \dots, z_n)^T$. This notation may occasionally be abused, but it should be clear from the context what the notation implies.

2.1. Singular perturbation reduction of linear, deterministic equations

In this subsection we consider linear perturbation equations of the form

$$\dot{x} = Ax + \varepsilon Bx, \quad x \in \mathbb{R}^n, \quad A, B \in \mathbb{R}^{n \times n}. \quad (2)$$

where A has a zero eigenvalue with algebraic and geometric multiplicity s , and $n - s$ real, nontrivial eigenvalues that are bounded above by $-\kappa$, where $0 < \kappa$. We will further assume that $A + \varepsilon B$ has n real eigenvalues that are strictly less than zero. Under these assumptions $x=0$ is a stable, hyperbolic equilibrium point of the perturbed system (2).

Due to its linearity, the solution to (2) is well-known

$$x(t) = e^{t(A + \varepsilon B)} x(0). \quad (3)$$

In most applications, we are only interested in the behavior of the solution after some initial transient, at which time the flow is *pushed* onto some low-dimensional subspace of \mathbb{R}^n (i.e., the slow eigenspace of $A + \varepsilon B$). The explicit computation of the eigenvalues and eigenvectors of $A + \varepsilon B$ can be cumbersome unless $A + \varepsilon B$ has a special structure (i.e., it is diagonal or triangular). To circumnavigate the need to work with the exact solution (3), we will invoke Fenichel theory, and exploit the fact that $0 < \varepsilon \ll 1$. To do this, set $\varepsilon = 0$ in (2) and observe that since the algebraic and geometric multiplicity of the zero eigenvalue is s we have

$$\mathbb{R}^n = \ker A \oplus \text{image } A = E^c \oplus E^s, \quad (4)$$

where E^c is the s -dimensional center subspace of A , and E^s is the $(n - s)$ -dimensional stable subspace of A . Both subspaces are invariant when $\varepsilon = 0$. Moreover, the flow restricted to E^c is trivial.

It is usually straightforward, especially for low-dimensional systems, to define a suitable N and W and express Ax in the form $NW^T x$, where the columns of N form a basis for the

range of A , the rows of W^T form a basis for the $\ker^\perp A$, and the critical manifold is given by the level set $W^T x = 0$. Given this factorization, the projections onto E^s and E^c are as follows:

$$\begin{aligned}\Pi^s &:= N(W^T N)^{-1} W^T : \mathbb{R}^n \mapsto \text{image } A = E^s \\ \Pi^c &:= \mathbb{I}^{n \times n} - N(W^T N)^{-1} W^T : \mathbb{R}^n \mapsto \ker A = E^c\end{aligned}$$

From Fenichel theory, the approximation³ to (2) on the slow timescale is

$$\frac{dx}{d\tau} = (\Pi^c B x)|_{x \in E^c}. \quad (6)$$

where $\tau = \varepsilon t$ is the slow time. Similarly, we can project (2) onto E^s

$$\frac{dx}{dt} = Ax|_{x \in E^s}. \quad (7)$$

Note that (6) is a linear system with s independent equations, and (7) contains $n - s$ independent equations. Formally, (6) is an approximation to (2) in the slow eigenspace, while (7) is an approximation to (2) in the fast eigenspace.

Singular perturbations come in two forms: standard and non-standard. When the system is in standard form, the first s components of x will be first integrals of the layer problem $\dot{x} = Ax$:

$$x_i = x_i(0), \quad 1 \leq i \leq s. \quad (8)$$

The components $x_i, i \leq s$ are called the slow variables since they do not change in the approach to E^c . In contrast, the remaining $n - s$ components, called the fast variables, change rapidly while the trajectory approaches the critical subspace.

Example 1. Consider the following two-dimensional system

$$\begin{pmatrix} \dot{x}_1 \\ \dot{x}_2 \end{pmatrix} = \begin{pmatrix} 0 & 0 \\ \mu & -\lambda \end{pmatrix} \begin{pmatrix} x_1 \\ x_2 \end{pmatrix} + \varepsilon \begin{pmatrix} -\alpha & \beta \\ 0 & 0 \end{pmatrix} \begin{pmatrix} x_1 \\ x_2 \end{pmatrix}, \quad (9)$$

which factors⁴ as

$$\begin{pmatrix} \dot{x}_1 \\ \dot{x}_2 \end{pmatrix} = \begin{pmatrix} 0 \\ 1 \end{pmatrix} (\mu x_1 - \lambda x_2) + \varepsilon \begin{pmatrix} -\alpha & \beta \\ 0 & 0 \end{pmatrix} \begin{pmatrix} x_1 \\ x_2 \end{pmatrix}, \quad (10)$$

The critical manifold is

$$S_0 = \{(x_1, x_2) \in \mathbb{R}^2 : f(x_1, x_2) = \mu x_1 - \lambda x_2 = 0\},$$

and the stable subspace, E^s , is

$$E^s := \{(x_1, x_2) \in \mathbb{R}^2 : x_1 = 0\}.$$

³This approximation will hold so long as Π^s is a good approximation to the projection onto the fast subspace of the unperturbed problem.

⁴In this example, N is the column vector $(0, 1)^T$ and W^T is the row vector $W^T = (\mu \ \lambda)$.

The projection matrices, Π^c and Π^s , are

$$\Pi^c := \begin{pmatrix} 1 & 0 \\ \mu/\lambda & 0 \end{pmatrix}, \quad \Pi^s := \begin{pmatrix} 0 & 0 \\ -\mu/\lambda & 1 \end{pmatrix},$$

and from (6) we obtain

$$x' = \left(\frac{\beta\mu}{\lambda} - \alpha \right) x := \lambda_s^{(1)} x \quad (11a)$$

$$y' = 0, \quad (11b)$$

where “ ’ ” denotes $d/d\tau$. Likewise, from (7) we obtain

$$\dot{x} = 0, \quad (12a)$$

$$\dot{y} = -\lambda y = \lambda_f^{(0)} y. \quad (12b)$$

It is important to emphasize that (11) and (12) approximate the flow on the fast and slow spaces of the perturbed problem corresponding to $0 < \varepsilon \ll 1$. The center and stable subspaces of the layer problem, E^c and E^s , may not be invariant with respect to the perturbed flow when $0 < \varepsilon$. Moreover, $\lambda_f^{(0)}$ and $\lambda_s^{(1)}$ are not the fast and slow eigenvalues, λ_f, λ_s of

$$\begin{pmatrix} -\varepsilon\alpha & \varepsilon\beta \\ \mu & -\lambda \end{pmatrix}.$$

They are in fact leading order approximations to λ_f and λ_s :

$$\lambda_f = \lambda_f(\varepsilon = 0) + \varepsilon \frac{d\lambda_f}{d\varepsilon} \Big|_{\varepsilon=0} + \mathcal{O}(\varepsilon^2) = \lambda + \varepsilon\lambda_f^{(1)} + \mathcal{O}(\varepsilon^2), \quad (13a)$$

$$\lambda_s = \lambda_s(\varepsilon = 0) + \varepsilon \frac{d\lambda_s}{d\varepsilon} \Big|_{\varepsilon=0} + \mathcal{O}(\varepsilon^2) = \varepsilon\lambda_s^{(1)} + \mathcal{O}(\varepsilon^2). \quad (13b)$$

Thus, the ratio

$$\frac{\varepsilon\lambda_s^{(1)}}{\lambda} = \frac{\varepsilon\lambda_s^{(1)}}{\lambda_f^{(0)}} \quad (14)$$

is a good approximation to λ_s/λ_f as long as ε is sufficiently small.

2.2. TFPV theory

Since our primary interest is in the reduction of differential equations that describe chemical reactions, it is important to discuss GSPT in the context of this specific application. The mass action equations that describe the temporal evolution of the concentrations of the participating chemical species are parameter-dependent and usually nonlinear:

$$\dot{x} = h(x, \pi), \quad x \in \mathbb{R}^n, \quad \pi \in \Lambda, \quad \Lambda \subseteq \mathbb{R}^m. \quad (15)$$

The validity of a particular set of reduced equations may depend not only on the magnitude of the eigenvalue disparity but also the *path* taken in parameter space that induces the disparity.

However, since the eigenvalues of the Jacobian matrix depend on the parameters of the reaction network (i.e., rate constants and conserved concentrations) there are usually *multiple* paths in parameter space that lead to eigenvalue disparity. Tikhonov-Fenichel Parameter Value (TFPV) theory removes some of this ambiguity by identifying critical parameter values associated with singular perturbation scenarios and their corresponding reductions [22, 23, 24]. Simply put, TFPV theory identifies *which* parameters must ultimately vanish in the singular limit for a specific reduction to hold. Briefly, given an m -tuple of parameters $\pi \in \mathbb{R}^m$, we call π^* a TFPV of dimension s if:

1. The zero level set $h(x, \pi^*) = 0$ is an s -dimensional submanifold of \mathbb{R}^n called the critical manifold, S_0 .
2. For each $x \in S_0$ there is a direct sum decomposition⁵

$$T_x \mathbb{R}^n \simeq \mathbb{R}^n = \ker D_1 h(x, \pi^*) \oplus \text{Im } D_1 h(x, \pi^*).$$

3. For each $x \in S_0$, the non-zero eigenvalues of $D_1 h(x, \pi^*)$ are strictly negative (this ensures the attractivity of the critical manifold).

Given a specific TFPV, we perturb the layer problem by perturbing π^* : $\pi = \pi^* + \varepsilon \rho$:

$$\dot{x} = h(x, \pi) = h(x, \pi^* + \varepsilon \rho) = h(x, \pi^*) + \varepsilon D_2(x, \pi) \rho + \dots = h^{(0)}(x, \pi^*) + \varepsilon h^{(1)}(x, \pi) + \dots \quad (16)$$

where “ D_2 ” denotes differentiation with respect to π . Once the system is expressed in perturbation form (16), we compute the reduced problem on S_0 by projecting the leading order perturbation, $h^{(1)}(x, \pi)$, onto the tangent space of S_0 . The zeroth-order term, $h^{(0)}(x, \pi^*)$, factors:

$$h^{(0)}(x, \pi^*) = P(x) \mu(x), \quad P(x) \in \mathbb{R}^{n \times n-s}, \quad \mu(x) \in \mathbb{R}^{n-s}. \quad (17)$$

The level set,

$$\mathcal{L} =: \{x \in \mathbb{R}^n : \mu(x) = 0\}$$

coincides with S_0 , and both $P(x)$ and $D\mu(x)$ have full rank on S_0 . Given the factorization (17), the reduced flow on S_0 is

$$\dot{x} = \varepsilon (I - P(x) (D\mu(x) P(x))^{-1} D\mu(x)) h^{(1)}(x, \pi). \quad (18)$$

Example 2. *As a didactic example, consider*



The mass action equations that describe the temporal dynamics of x, y , and z (the respective concentrations of X, Y , and Z) are:

$$\dot{x} = -k_1 x + k_2 y, \quad (20a)$$

$$\dot{y} = k_1 x - (k_2 + k_3) y. \quad (20b)$$

⁵ D_1 denotes differentiation with respect to x .

The parameters $(k_1, k_2, k_3)^T$ lie in a subset of $\mathbb{R}_{\geq 0}^3$. Consider $\pi^* = (0, k_2, k_3)^T$ where k_2 and k_3 are bounded above and below by positive constants. The system (20) reduces to

$$\begin{aligned}\dot{x} &= k_2 y, \\ \dot{y} &= -(k_2 + k_3)y,\end{aligned}$$

and by inspection one sees that $y = 0$ is a critical invariant manifold comprised of non-isolated equilibria. The Jacobian, $D_1 h(z, \pi^*)$ along $S_0 := \{(x, y) \in \mathbb{R}^2 : y = 0\}$ is

$$D_1 h(z, \pi^*) = D_1 h^{(0)}(z, \pi^*) = \begin{pmatrix} 0 & k_2 \\ 0 & -(k_2 + k_3) \end{pmatrix}$$

and therefore $\pi^* = (0, k_2, k_3)^T$ is a TFPV and

$$h^{(0)}(z, \pi^*) =: \begin{pmatrix} k_2 \\ -(k_2 + k_3) \end{pmatrix} \cdot y = P(z) \cdot \mu(z), \quad z = (x, y).$$

To perturb the layer problem (21) we perturb π^* in the direction of k_1 :

$$\pi := \begin{pmatrix} 0 \\ k_2 \\ k_3 \end{pmatrix} + \varepsilon \begin{pmatrix} k_1 \\ 0 \\ 0 \end{pmatrix} =: \pi^* + \varepsilon \rho \tag{22}$$

and therefore

$$\varepsilon h^{(1)}(z, \pi) = \varepsilon \begin{pmatrix} -x & y & 0 \\ x & -y & -y \end{pmatrix} \cdot \begin{pmatrix} k_1 \\ 0 \\ 0 \end{pmatrix} = \varepsilon k_1 \begin{pmatrix} -1 \\ 1 \end{pmatrix}. \tag{23}$$

Consequently, there exists a unique projection matrix, $\Pi^c : \mathbb{R}^2 \mapsto T_z S_0$

$$\Pi^c = (I - P(x) (D\mu(x)P(x))^{-1} D\mu(x)) = \begin{pmatrix} 1 & \frac{k_2}{k_2 + k_3} \\ 0 & 0 \end{pmatrix}.$$

The reduced equation, valid on the slow time scale, is thus given by

$$\begin{pmatrix} x' \\ y' \end{pmatrix} = k_1 x \begin{pmatrix} 1 & \frac{k_2}{k_2 + k_3} \\ 0 & 0 \end{pmatrix} \begin{pmatrix} -1 \\ 1 \end{pmatrix} = \begin{pmatrix} -\frac{k_1 k_3}{k_2 + k_3} \\ 0 \end{pmatrix} x$$

where again “ ’ ” denotes differentiation with respect to the slow time, $\tau = \varepsilon t$.

The reduction⁶

$$x' = -\frac{k_1 k_3}{k_2 + k_3} x \tag{24}$$

is good to an arbitrary degree of accuracy as $k_1 \rightarrow 0$ with all other parameters bounded above and below by positive constants. From an applied perspective, TFPV theory does not say *how small* k_1 must be in comparison to the remaining parameters. There is an obvious connection to eigenvalue disparity in this question, and recent work has made progress in this direction; see [27].

⁶Of course, one needs to supply (24) with an initial condition, and this can be done by computing the intersection of the first integral with the critical manifold; see [7, 25] for details.

2.3. The ssLNA: Derivation via singular perturbation methods

In the thermodynamic limit, the temporal evolution of the concentrations of the chemical species, x_i , that participate in a reaction network are governed by a nonlinear ODE (15). Assume that $h(x; \pi)$ admits an isolated stationary point at $x = x^*$ that is both hyperbolic and attracting. Since stochastic fluctuations persist near the thermodynamic limit, it is necessary to consider the random fluctuations about the mean, $x = x^*$. Let X_i denote the randomly fluctuating departure from the mean field concentration x_i^* (i.e., the steady-state concentration of species x_i), where n_i is the (randomly fluctuating) number of molecules of species “ i ”. The LNA presents the temporal evolution of X as an Ornstein-Uhlenbeck process:

$$dX = JXdt + GdW, \quad G := \Omega^{-1/2}(\mathcal{S}\sqrt{F})|_{x=x^*} \quad (25)$$

where $W_i(\cdot)$ are independent Brownian motions, \mathcal{S} is a stoichiometric matrix, and F is a diagonal matrix whose elements are the macroscopic rates of each elementary reaction under steady-state conditions.

The solution to (25)

$$X(t) = e^{tJ}X_0 + \Omega^{-1/2} \int_0^t e^{(t-t')J}G dW(t'),$$

is well-understood: the expectation, $\mathbb{E}(X)$, is given by

$$\mathbb{E}(X) = e^{tJ}\mathbb{E}(X_0) \quad (26)$$

and, in the long-time limit, the covariance matrix, $C_{\mathcal{V}}$, satisfies the Lyapunov equation

$$JC_{\mathcal{V}} + C_{\mathcal{V}}J^T = -\Omega^{-1}\mathcal{S}F\mathcal{S}^T =: \Omega^{-1}\tilde{G}, \quad (27)$$

which admits the solution

$$C_{\mathcal{V}} = \Omega^{-1} \int_0^\infty e^{tJ}\tilde{G}e^{tJ^T} dt.$$

When the Jacobian matrix, J , has disparate eigenvalues, further reduction of the LNA is possible via the ssLNA. Assume that J is expressible in terms of the sum

$$J = A + \varepsilon B$$

with $\dim \ker A = s$. In perturbation form, the LNA is

$$dX = (A + \varepsilon B)Xdt + GdW. \quad (28)$$

Passing *two* limits

- Let $\varepsilon \rightarrow 0$ (the singular limit),
- Let $\Omega \rightarrow \infty$ (the thermodynamic limit),

generates a linear dynamical system,

$$\dot{X} = AX$$

with a normally hyperbolic critical manifold, $S_0 := \{(X_1, X_2) \in \mathbb{R}^n : AX = 0\}$. The corresponding ssLNA is

$$dX = \varepsilon(\Pi^c BX|_{X \in E^c})dt + \Pi^c GdW. \quad (29)$$

Thus, the ssLNA is fundamentally the projection (restriction) of the LNA onto the nullspace of A . The ssLNA was originally derived for systems in, or presumed to be in, standard form [19, 18, 17, 28, 29]. However, the accuracy of (29) as a reduction when the underlying singular perturbation problem is not in standard form remains unclear. Specifically, it is unclear if the variance obtained from (29) accurately approximates the variance of (28) in a general sense. At the Langevin level, the answer to this question has already partially been answered. Katzenberger [30], and later Parsons and Rogers [31] noted that a straightforward projection onto the critical manifold is not enough to produce a reduced model, since the curvature of the critical manifold and or the curvature of the flow field can induce a stochastic drift. However, the drift term is typically $\mathcal{O}(\Omega^{-1})$, and can thus presumably be discarded in the realm of the LNA. This raises the question: is projection onto a critical manifold enough to secure a useful reduced model near the thermodynamic limit? The answer to this question is the subject of Section 3.

3. Breaking down the noise: The fast scale linear noise approximation

To understand the relationship between timescale separation and the reduction of the LNA, it will be extremely useful to define the *fast scale linear noise approximation* (fsLNA) as follows:

$$dX = \Pi^s A|_{X \in E^s} dt + \Pi^s GdW, \quad (30)$$

which is the projection of (28) onto the fast (stable) subspace of A .

To derive an explicit relationship between the eigenvalue ratio (timescale ratio) and the variance of X , the form of the underlying singular perturbation problem matters. We will illustrate this by considering the standard form in two dimensions, but we remark that the two-dimensional results easily extend to higher-dimensional systems. To start, let

$$\begin{aligned} X_1 &:= \text{slow variable,} \\ X_2 &:= \text{fast variable.} \end{aligned}$$

In standard form, the drift term AX is identically

$$AX := \begin{pmatrix} 0 \\ 1 \end{pmatrix} W^T X = NW^T X, \quad N \in \mathbb{R}^{2 \times 1} \quad W^T \in \mathbb{R}^{1 \times 2}.$$

The critical manifold is the level set

$$S_0 := \{(X_1, X_2) \in \mathbb{R}^2 : W^T X = 0\},$$

which is an 1-dimensional submanifold of \mathbb{R}^n . Let $f(X_1, X_2)$ denote $W^T X$. The projection matrix, Π^c , is

$$\Pi^c := \begin{pmatrix} 1 & 0 \\ -(\partial_{X_2} f(X))^{-1} \partial_{X_1} f(X) & 0 \end{pmatrix}. \quad (32)$$

From the structure of the projection matrix we have the following:

Proposition 1. *Suppose the layer problem associated with (28) defines a linear, singularly perturbed ODE system in standard form such that X_1 is the slow variable and X_2 is the fast variable. The one-dimensional fsLNA to the slow variable, X_1 , is, to leading order in ε , identically zero.*

Proof. The projection matrix Π^s is

$$\Pi^s := \begin{pmatrix} 0 & 0 \\ (\partial_{X_2} f(X))^{-1} \partial_{X_1} f(X) & 1 \end{pmatrix}. \quad (33)$$

The fsLNA is

$$dX = \Pi^s A X|_{X \in E^s} + \Pi^s G dW$$

and therefore

$$dX_1 = 0. \quad (34)$$

□

Since (34) is completely deterministic, the variance of the slow variable, X_1 , is zero. Thus, the dominant contribution to the noise is due to the slow scale and, consequently, the variance of the slow variable obtained from the ssLNA (29) will be in very good agreement with the variance of the LNA. Specifically, when the system is planar and in standard form, the variances generated by the LNA and the ssLNA differ by terms that are $\mathcal{O}(\varepsilon)$.

Proposition 2. *Let \mathbb{V}_{LNA} denote the long-time variance of X_1 for a (1, 1) fast/slow system in standard form:*

$$\begin{pmatrix} dX_1 \\ dX_2 \end{pmatrix} = \begin{pmatrix} \varepsilon J_{ss} & \varepsilon J_{sf} \\ J_{fs} & J_{ff} \end{pmatrix} \begin{pmatrix} X_1 \\ X_2 \end{pmatrix} dt + G dW, \quad (35)$$

and let \mathbb{V}_{ssLNA} denote the long-time variance of X_1 obtained from the ssLNA to (35). It holds that

$$|\mathbb{V}_{LNA} - \mathbb{V}_{ssLNA}| \sim \mathcal{O}(\varepsilon). \quad (36)$$

Proof. Let J denote

$$\begin{pmatrix} \varepsilon J_{ss} & \varepsilon J_{sf} \\ J_{fs} & J_{ff} \end{pmatrix}.$$

The long-time variance of X_1 is given by the solution to the continuous-time Lyapunov equation,

$$JV + VJ^T = -GG^T, \quad \text{where} \quad \lim_{t \rightarrow \infty} \mathbb{V}(X_1) = V(1, 1),$$

which is equivalent to the linear matrix/vector equation

$$[(I \otimes J) + (J \otimes I)] \text{vec}(V) = -\text{vec}(GG^T). \quad (37)$$

Let \tilde{G} denote⁷

$$-\text{vec}(GG^T) = -\text{vec}(\tilde{G}) =: \begin{pmatrix} \tilde{G}_{ss} \\ \tilde{G}_{fs} \\ \tilde{G}_{sf} \\ \tilde{G}_{ff} \end{pmatrix}.$$

The first component, $V(1, 1)$, of the exact solution to (37) is

$$\frac{\varepsilon^2 J_{sf} \tilde{G}_{ff} + (((\tilde{G}_{fs} + \tilde{G}_{sf}) J_{sf} - \tilde{G}_{ss} J_{ss}) J_{ff} + \tilde{G}_{ss} J_{fs} J_{sf}) \varepsilon - \tilde{G}_{ss} J_{ff}^2}{2\varepsilon(\varepsilon J_{ss} + J_{ff})(J_{ff} J_{ss} - J_{fs} J_{sf})} = -\frac{\tilde{G}_{ss} J_{ff}}{2\varepsilon(J_{ss} J_{ff} - J_{fs} J_{sf})} + \mathcal{O}(\varepsilon), \quad (38)$$

where $\tilde{G}_{ss} > 0$, $J_{ff} < 0$ and $0 < \det J$. The long-time variance of X_1 obtained from the ssLNA is

$$-\frac{\tilde{G}_{ss} J_{ff}}{2\varepsilon(J_{ss} J_{ff} - J_{fs} J_{sf})} \quad (39)$$

and the assertion (36) follows. \square

Thus, in standard form, timescale separation (eigenvalue disparity) is enough to ensure that the variance of the ssLNA is an extremely good approximation to the slow variable variance obtained from the LNA as $\varepsilon \rightarrow 0$. However, the following example illustrates that this is not necessarily true when the system is not in standard form.

Example 3. Consider a planar (1, 1) fast/slow system

$$\begin{pmatrix} dX_1 \\ dX_2 \end{pmatrix} = \begin{pmatrix} -a_{11} & a_{12} \\ a_{11} & -a_{12} \end{pmatrix} \begin{pmatrix} X_1 \\ X_2 \end{pmatrix} dt + \varepsilon \begin{pmatrix} 0 & 0 \\ 0 & -b_{22} \end{pmatrix} \begin{pmatrix} X_1 \\ X_2 \end{pmatrix} dt + GdW,$$

with $a_{ij} > 0$ and $b_{22} > 0$. The critical manifold is

$$S_0 := \{X \in \mathbb{R}^2 : -a_{11}X_1 + a_{12}X_2 = 0\}, \quad (40)$$

which is parameterizable in terms of X_1 or X_2 . Neither variable is slow. However, it is possible to construct reduced equations for X_1 or X_2 . We will work with X_1 .

$$dX_1^s = -\frac{\varepsilon b_{11} a_{11}}{a_{11} + a_{12}} X_1^s dt + \sum_j (\Pi^c G)_{1j} dW_j, \quad (41)$$

where once again

$$-\frac{\varepsilon b_{11} a_{11}}{a_{11} + a_{12}} = \varepsilon \lambda_s^{(1)}.$$

⁷Note that $\tilde{G}_{ss} = \sum_j (S\sqrt{F})_{1j}^2$.

The variance obtained from the ssLNA (41) is:

$$\lim_{t \rightarrow \infty} \mathbb{V}(X_1^s) = \frac{1}{2\Omega} \cdot \sum_j (\Pi^c G)_{1j}^2 \cdot \frac{1}{|\varepsilon \lambda_s^{(1)}|}. \quad (42)$$

It is equally important to consider the projection onto the stable subspace. On the fast timescale we have,

$$dX_1^f = \lambda_f^{(0)} \cdot X_1^f dt + \sum_j (\Pi^s G)_{1j} dW_j. \quad (43)$$

The variance obtained from the fsLNA is

$$\lim_{t \rightarrow \infty} \mathbb{V}(X_1^f) = \frac{1}{2\Omega} \cdot \sum_j (\Pi^s G)_{1j}^2 \cdot \frac{1}{|\lambda_f^{(0)}|}. \quad (44)$$

In practice, the hope is generally to be able to use the ssLNA (41) in place of the full LNA and still recover an accurate approximation to the variance. However, to recover an accurate approximation to the variance of X_1 using only the ssLNA, it is desirable that

$$\lim_{t \rightarrow \infty} \frac{\mathbb{V}(X_1^f)}{\mathbb{V}(X_1^s)} = \frac{|\varepsilon \lambda_s^{(1)}|}{|\lambda_f^{(0)}|} \cdot \frac{\sum_j (\Pi^s G)_{1j}^2}{\sum_j (\Pi^c G)_{1j}^2} =: \delta \ll 1. \quad (45)$$

While $\varepsilon \rightarrow 0$ ensures that the ratio of slow and fast timescales (eigenvalues) vanishes, δ may not vanish in the singular limit:

$$\lim_{\varepsilon \rightarrow 0} \frac{|\varepsilon \lambda_s^{(1)}|}{|\lambda_f^{(0)}|} = 0 \not\Rightarrow \lim_{\varepsilon \rightarrow 0} \delta = 0. \quad (46)$$

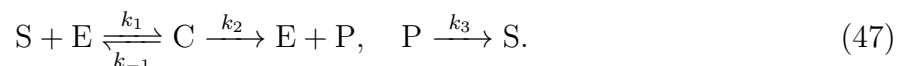
Hence, the ssLNA does not automatically ensure an accurate estimation of the variance when the system is not in standard form, and we can conclude that non-standard systems may require a case-by-case analysis.

4. Case Studies

In this section we present several case studies of dynamical systems that emerge from biochemical reactions and illustrate the relationship between the ssLNA derived from singular perturbation theory and its efficacy in the vicinity of a stationary point. For simplicity, and because we have chosen to work in arbitrary units, we set $\Omega = 1$.

4.1. The non-standard form: slow product formation and degradation

We first consider the Michaelis-Menten reaction with feedback:



The mass action equations that describe the temporal dynamics of (47) in the thermodynamic limit are

$$\dot{s} = -k_1(e_0 - c)s + k_{-1}c + k_3(s_0 - s - c), \quad (48a)$$

$$\dot{c} = k_1(e_0 - c)s - (k_{-1} + k_2)c, \quad (48b)$$

where s and c denote the respective concentrations of S and C and e_0 and s_0 are the initial concentrations of E and S . Observe that (48) admits stationary point⁸ located at $(s, c) = (s_{ss}, c_{ss})$, and depends on the parameters $\pi =: (k_1, k_2, k_3, k_{-1}, e_0, s_0)^T$. The TFPV of interest is

$$\pi^* := (k_1, 0, 0, k_{-1}, e_0, s_0)^T$$

and, since we are interested in the slow time behavior of (48) with parameter values near π^* , we rescale $k_2 \mapsto \varepsilon k_2$ and $k_3 \mapsto \varepsilon k_3$:

$$\dot{s} = -k_1(e_0 - c)s + k_{-1}c + \varepsilon k_3(s_0 - s - c), \quad (49a)$$

$$\dot{c} = k_1(e_0 - c)s - k_{-1}c - \varepsilon k_2c. \quad (49b)$$

The system (49) admits an infinite number of stationary points in the singular limit:

$$S_0 := \{(s, c) \in \mathbb{R}^2 : \phi(s, c) = 0\} \cap \{(s, c) \in \mathbb{R}^2 : 0 \leq s \leq s_0 \ \& \ 0 \leq c \leq \min\{e_0, s_0\}\},$$

where $\phi(s, c) : \mathbb{R}^2 \mapsto \mathbb{R}^1 = k_1(e_0 - c)s - k_{-1}c$. The level set $\phi(s, c) = 0$ is a submanifold of \mathbb{R}^2 that is also normally hyperbolic and attracting. In perturbation form we have

$$\begin{pmatrix} \dot{s} \\ \dot{c} \end{pmatrix} = \begin{pmatrix} -1 \\ 1 \end{pmatrix} \phi(s, c) + \varepsilon \begin{pmatrix} k_3(s_0 - s - c) \\ -k_2c \end{pmatrix}, \quad (50)$$

and the reduced equation that describes the evolution of s on the slow timescale, $\tau = \varepsilon t$, is

$$\begin{pmatrix} s' \\ c' \end{pmatrix} = \begin{pmatrix} 1 - \varphi(s, c) & \zeta(s, c) \\ \varphi(s, c) & 1 - \zeta(s, c) \end{pmatrix} \begin{pmatrix} k_3(s_0 - s - c) \\ -k_2c \end{pmatrix} \Big|_{c=e_0s/(K_S+s)} \quad (51)$$

where $\varphi(s, c)$ and $\zeta(s, c)$ are:

$$\varphi(s, c) =: \frac{(e_0 - c)}{(e_0 - c) + (s + K_S)}, \quad \zeta(s, c) =: \frac{(s + K_S)}{(e_0 - c) + (s + K_S)}.$$

The reduced equation for s is

$$s' = \frac{k_3(s + K_S)^2}{e_0K_S + (s + K_S)^2} \left(s_0 - s - \frac{e_0s}{K_S + s} \right) - \frac{Vs(s + K_S)}{e_0K_S + (s + K_S)^2}, \quad V =: k_2e_0, \quad (52)$$

and is valid in the limit of small k_2 and k_3 .

⁸The exact expressions for s_{ss} and c_{ss} are not integral to the analysis and we have therefore chosen to omit them.

In the presence of intrinsic noise, and under steady-state conditions⁹, the LNA associated with (48) is the Ornstein–Uhlenbeck process:

$$\begin{pmatrix} dX_s \\ dX_c \end{pmatrix} = k_1 \begin{pmatrix} -(e_0 - c_{ss}) & (s_{ss} + K_S) \\ (e_0 - c_{ss}) & -(s_{ss} + K_S) \end{pmatrix} \begin{pmatrix} X_s \\ X_c \end{pmatrix} dt + \varepsilon \begin{pmatrix} -k_3 & -k_3 \\ 0 & -k_2 \end{pmatrix} \begin{pmatrix} X_s \\ X_c \end{pmatrix} dt + G dW, \quad (53)$$

with

$$G = \begin{pmatrix} -\sqrt{k_1(e_0 - c_{ss})s_{ss}} & \sqrt{k_{-1}c_{ss}} & 0 & \sqrt{\varepsilon k_3(s_0 - s_{ss} - c_{ss})} \\ \sqrt{k_1(e_0 - c_{ss})s_{ss}} & -\sqrt{k_{-1}c_{ss}} & -\sqrt{\varepsilon k_2 c_{ss}} & 0 \end{pmatrix} \quad (54)$$

and $dW = (dW_1 \ dW_2 \ dW_3 \ dW_4)^T$. To formulate the ssLNA, we construct the projection operators that map \mathbb{R}^2 onto the invariant subspaces of A :

$$A := \begin{pmatrix} -(e_0 - c_{ss}) & (s_{ss} + K_S) \\ (e_0 - c_{ss}) & -(s_{ss} + K_S) \end{pmatrix},$$

which are as follows:

$$\Pi^c := \begin{pmatrix} 1 - \varphi(s_{ss}, c_{ss}) & \zeta(s_{ss}, c_{ss}) \\ \varphi(s_{ss}, c_{ss}) & 1 - \zeta(s_{ss}, c_{ss}) \end{pmatrix}, \quad \Pi^s := \begin{pmatrix} \varphi(s_{ss}, c_{ss}) & -\zeta(s_{ss}, c_{ss}) \\ -\varphi(s_{ss}, c_{ss}) & \zeta(s_{ss}, c_{ss}) \end{pmatrix}. \quad (55)$$

It is straightforward to compute δ and show that $\lim_{\varepsilon \rightarrow 0} \delta \neq 0$ as $\varepsilon \rightarrow 0$. Consequently, one cannot rely on the ssLNA to recover the appropriate variance for X_s ; see FIG 2.

4.2. Standard form: The total QSSA

We now ask whether or not a coordinate transformation will improve the situation encountered in the previous subsection? The answer, as we will show, is certainly yes: a transformation into standard form will dramatically improve the ability of the ssLNA to approximate the variance.

To transform (49) into standard form note that when $k_2 = k_3 = 0$, the *total substrate* concentration, $s_T = s + c$ is a conserved quantity (first integral) since

$$\dot{s} + \dot{c} = 0.$$

The total substrate concentration was first utilized in the deterministic regime by Borghans et al. [32], and has been found to be quite useful in the stochastic realm as well; see [33] for a nice review concerning the utility of s_T in stochastic modeling.

In the limit of small k_2 and k_3 , the slow variable is s_T , not s . Rewriting the mass action equations in terms of s_T and c yields a singularly perturbed system in standard form:

$$\dot{s}_T = -\varepsilon k_2 c + \varepsilon k_3 (s_0 - s_T), \quad (56a)$$

$$\dot{c} = k_1 (e_0 - c)(s_T - c) - k_{-1} c - \varepsilon k_2 c. \quad (56b)$$

The critical manifold is

$$S_0 := \{(s_T, c) \in \mathbb{R}^2 : 2c = e_0 + K_S + s_T - \sqrt{(e_0 + K_S + s_T)^2 - 4e_0 s_T}\} \cap \Delta,$$

⁹The exact expressions for s_{ss} and c_{ss} depend on k_2 and k_3 and therefore on ε . However, s_{ss} and c_{ss} are $\mathcal{O}(1)$.

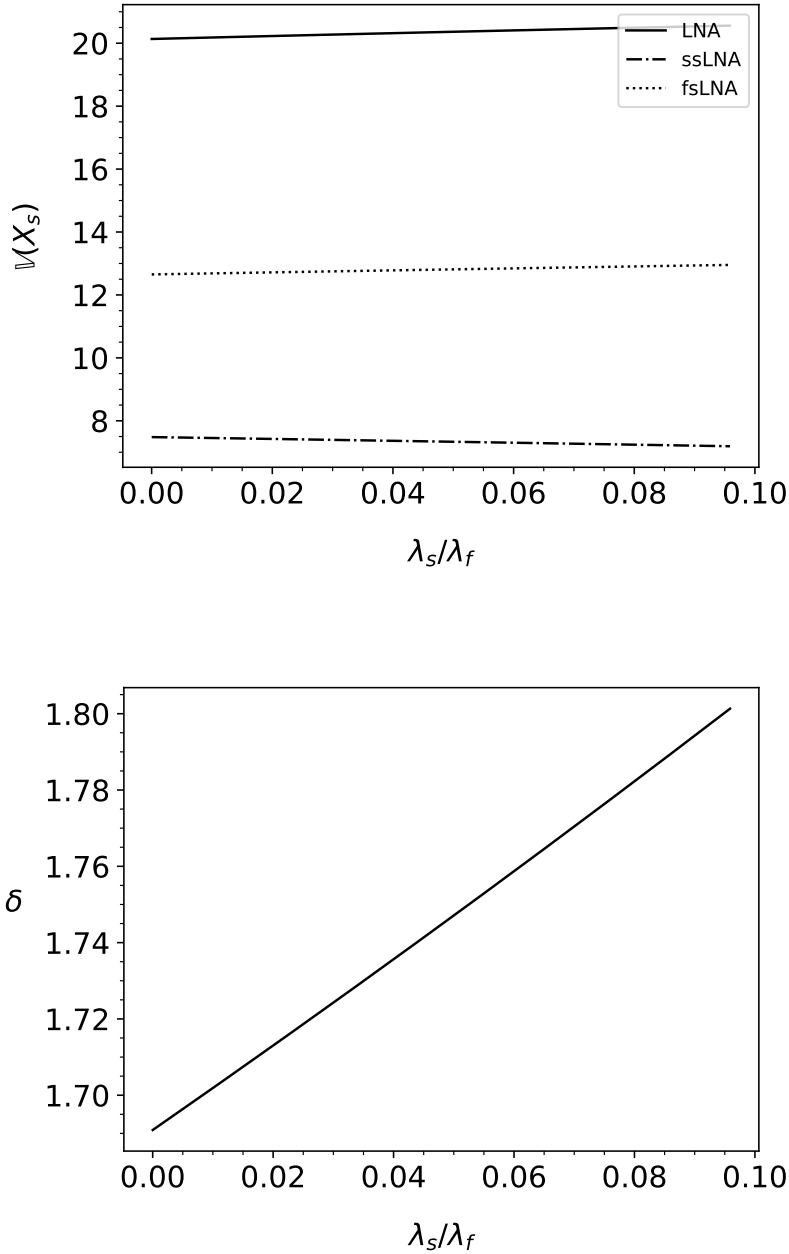


Figure 2: **The ssLNA may not generate a good approximation to the variance when the dynamical system is not in standard form.** TOP panel: The variances of X_s obtained from the LNA, the ssLNA, and *fs*LNA. Note that the ssLNA underestimates $\mathbb{V}(X_s)$ by roughly 60% and that it does not improve as the eigenvalue ratio (timescale separation) vanishes. BOTTOM panel: δ versus λ_s/λ_f . Note that the δ remains of order unity even as $\lambda_s/\lambda_f \rightarrow 0$. All calculations were computed with the following parameter values (in arbitrary units): $k_1 = 1.0, e_0 = s_0 = 100.0, k_{-1} = 50.0; k_2 = k_3 = \varepsilon$ and ε is varied from 10 to 10^{-3} .

where $\Delta = \{(s_T, c) \in \mathbb{R}^2 : 0 \leq s_T \leq s_0 \ \& \ 0 \leq c \leq \min\{e_0, s_0\}\}$. The reduced equation for

s_T is

$$s'_T = -\frac{1}{2}k_2 \left(e_0 + K_S + s_T - \sqrt{(e_0 + K_S + s_T)^2 - 4e_0s_T} \right) + k_3(s_0 - s_T). \quad (57)$$

The rate equations in fast/slow coordinates (56) admit a stationary point at $(s_T, c) = (s_T^{ss}, c_{ss})$. The LNA is

$$\begin{aligned} \begin{pmatrix} dX_T \\ dX_c \end{pmatrix} &= \begin{pmatrix} 0 & 0 \\ k_1(e_0 - c_{ss}) & -k_1(s_T^{ss} + e_0 + K_S) + 2k_1c_{ss} \end{pmatrix} \begin{pmatrix} X_T \\ X_c \end{pmatrix} dt \\ &+ \varepsilon \begin{pmatrix} -k_3 & -k_2 \\ 0 & -k_2 \end{pmatrix} \begin{pmatrix} X_T \\ X_c \end{pmatrix} + GdW, \end{aligned} \quad (58)$$

with G given by

$$G := \begin{pmatrix} 0 & 0 & -\sqrt{\varepsilon k_2 c_{ss}} & \sqrt{\varepsilon k_3 (s_0 - s_T^{ss})} \\ \sqrt{k_1(e_0 - c_{ss})(s_T^{ss} - c_{ss})} & -\sqrt{k_{-1}c_{ss}} & -\sqrt{\varepsilon k_2 c_{ss}} & 0 \end{pmatrix}. \quad (59)$$

The critical manifold that emerges in the singular and thermodynamic limits is

$$S_0 := \{(X_T, X_c) \in \mathbb{R}^2 : (e_0 - c_{ss})X_T - (s_T^{ss} + e_0 + K_S - 2c_{ss})X_c = 0\},$$

and the projection matrices, Π^c and Π^s are

$$\Pi^c = \begin{pmatrix} 1 & 0 \\ \frac{e_0 - c_{ss}}{s_T^{ss} + e_0 + K_S - 2c_{ss}} & 0 \end{pmatrix}, \quad \Pi^s = \begin{pmatrix} 0 & 0 \\ -\frac{e_0 - c_{ss}}{s_T^{ss} + e_0 + K_S - 2c_{ss}} & 1 \end{pmatrix}.$$

The ssLNA for X_T is thus

$$dX_T = -\varepsilon \left(k_3 + \frac{k_2(e_0 - c_{ss})}{s_T^{ss} + e_0 + K_S - 2k_1c_{ss}} \right) X_T + \sqrt{\varepsilon k_3 (s_0 - s_T^{ss})} dW_4 - \sqrt{\varepsilon k_2 c_{ss}} dW_3. \quad (60)$$

Moreover, and most importantly, the *fs*LNA for X_T is trivial:

$$dX_T = 0. \quad (61)$$

This example illustrates why a transformation to standard form (when tractable) increases the accuracy of the variance obtained from the ssLNA; see FIG 3.

4.3. Non-standard form: low enzyme concentration

As a final example of this section we again consider (47) but this time consider small e_0 and small k_3 :

$$\dot{s} = -k_1(\varepsilon e_0 - c)s + k_{-1}c + \varepsilon k_3(s_0 - s - c), \quad (62a)$$

$$\dot{c} = k_1(\varepsilon e_0 - c)s - k_{-1}c - k_2c, \quad (62b)$$

with corresponding TFPV

$$\pi^* := (k_1, k_2, 0, k_{-1}, 0, s_0)^T.$$

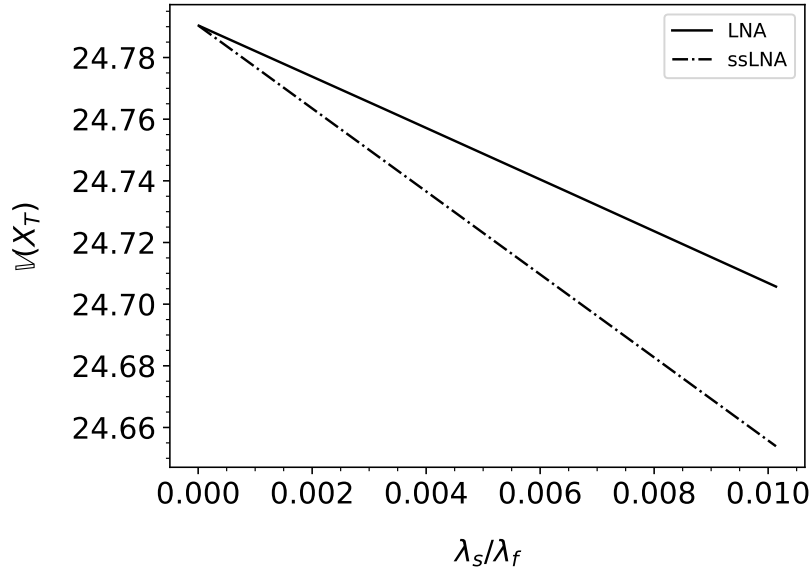


Figure 3: **A transformation to standard form can improve the accuracy of the variance obtained from ssLNA.** TOP panel: The variances of X_T obtained from the LNA, the ssLNA, and fs LNA. Note that the variance predicted by the ssLNA approaches the variance of the LNA as $\lambda_s/\lambda_f \rightarrow 0$. All calculations were computed with the following parameter values (in arbitrary units): $k_1 = 1.0, e_0 = s_0 = 100.0, k_{-1} = 50.0; k_2 = k_3 = \varepsilon$ and ε is varied from 1.0 to 10^{-3} .

In the singular limit obtained by setting $\varepsilon = 0$ we obtain a normally hyperbolic and compact critical manifold

$$S_0 := \{(s, c) \in \mathbb{R}^2 : c = 0\} \cap \Delta.$$

The reduction obtained via projection onto $T_x S_0$ is

$$s' = -\frac{Vs}{K_M + s} + k_3(s_0 - s). \quad (63)$$

Remark 1. *It is a common misconception that the standard quasi-steady-state approximation,*

$$s' = -\frac{Vs}{K_M + s}$$

and its variations (63) result from a singular perturbation in standard form. In fact this is not the case and an explanation for this phenomenon (which is far from self-evident, and holds only when special conditions are satisfied) is given in [23, Proposition 5]. In addition, rigorous requirements for the validity of scaling laws in such cases can be found in [34].

The system (62) has a stationary point located at $(s, c) = (s_{eq.}, c_{eq.})$, where

$$c_{eq.} = \frac{\varepsilon e_0 s_{eq.}}{K_M + s_{eq.}}, \quad K_M := \frac{k_{-1} + k_2}{k_1}. \quad (64)$$

Remark 2. Note that $c_{eq.} \rightarrow 0$ as $\varepsilon \rightarrow 0$. This is important and distinct from the previous examples. As a reminder that $c_{eq.} \sim \mathcal{O}(\varepsilon)$ we will write $c_{eq.} = \varepsilon \widehat{c}_{eq.}$.

The Jacobian evaluated at the stationary point is

$$J = \begin{pmatrix} -\varepsilon k_1(e_0 - \widehat{c}_{eq.}) - \varepsilon k_3 & k_1 s_{eq.} + k_{-1} - \varepsilon k_3 \\ \varepsilon k_1(e_0 - \widehat{c}_{eq.}) & -k_1 s_{eq.} - k_{-1} - k_2 \end{pmatrix},$$

and therefore we can express the Jacobian as $J = A + \varepsilon B$ with

$$A = \begin{pmatrix} 0 & k_1 s_{eq.} + k_{-1} \\ 0 & -k_1 s_{eq.} - k_{-1} - k_2 \end{pmatrix}, \quad B = \begin{pmatrix} -k_1(e_0 - \widehat{c}_{eq.}) - k_3 & -k_3 \\ k_1(e_0 - \widehat{c}_{eq.}) & 0 \end{pmatrix}. \quad (65)$$

From A we see that the critical manifold, S_0 is

$$S_0 := \{(X_s, X_c) \in \mathbb{R}^2 : X_c = 0\},$$

and we proceed to compute Π^c and Π^s :

$$\Pi^c := \begin{pmatrix} 1 & \frac{s_{eq.} + K_S}{s_{eq.} + K_M} \\ 0 & 0 \end{pmatrix}, \quad \Pi^s := \begin{pmatrix} 0 & -\frac{s_{eq.} + K_S}{s_{eq.} + K_M} \\ 0 & 1 \end{pmatrix}. \quad (66)$$

The LNA that corresponds to small e_0 and small k_3 is

$$\begin{pmatrix} dX_s \\ dX_c \end{pmatrix} = (A + \varepsilon B) \begin{pmatrix} X_s \\ X_c \end{pmatrix} dt + G dW, \quad (67)$$

where A and B are given by (65) and G is

$$G = \begin{pmatrix} -\sqrt{k_1 \varepsilon (e_0 - \widehat{c}_{eq.}) s_{eq.}} & \sqrt{k_{-1} \varepsilon \widehat{c}_{eq.}} & 0 & \sqrt{\varepsilon k_3 (s_0 - s_{eq.} - \varepsilon \widehat{c}_{eq.})} \\ \sqrt{k_1 \varepsilon (e_0 - \widehat{c}_{eq.}) s_{eq.}} & -\sqrt{k_{-1} \varepsilon \widehat{c}_{eq.}} & -\sqrt{k_2 \varepsilon \widehat{c}_{eq.}} & 0 \end{pmatrix}. \quad (68)$$

The resulting ssLNA is

$$\begin{aligned} dX_s = & -\varepsilon \left(\frac{VK_M}{(K_M + s_{eq.})^2} + k_3 \right) X_s dt \\ & - \frac{K}{K_M + s_{eq.}} \left(\sqrt{k_1 \varepsilon (e_0 - \widehat{c}_{eq.}) s_{eq.}} dW_1 - \sqrt{k_{-1} \varepsilon \widehat{c}_{eq.}} dW_2 \right) \\ & - \left(\frac{s_{eq.} + K_S}{s_{eq.} + K_M} \right) \sqrt{k_2 \varepsilon \widehat{c}_{eq.}} dW_3 + \sqrt{\varepsilon k_3 (s_0 - s_{eq.} - \varepsilon \widehat{c}_{eq.})} dW_4, \end{aligned} \quad (69)$$

where $K := k_2/k_1$. The corresponding fsLNA is

$$\begin{aligned} dX_s = & -k_1(s_{eq.} + K_M)X_s dt \\ & + \left(\frac{s_{eq.} + K_S}{s_{eq.} + K_M} \right) \left(\sqrt{k_{-1} \varepsilon \widehat{c}_{eq.}} dW_2 + \sqrt{k_2 \varepsilon \widehat{c}_{eq.}} dW_3 - \sqrt{k_1 \varepsilon (e_0 - \widehat{c}_{eq.}) s_{eq.}} dW_1 \right). \end{aligned} \quad (70)$$

Observe that the limit

$$\lim_{\varepsilon \rightarrow 0} \frac{\varepsilon \left(\frac{VK_M}{(K_M + s_{eq.})^2} + k_3 \right)}{k_1(s_{eq.} + K_M)} = 0,$$

which is the leading order approximation to the eigenvalue ratio of the full Jacobian at the stationary point, clearly vanishes as $\varepsilon \rightarrow 0$. Moreover, $\delta \rightarrow 0$ as $\varepsilon \rightarrow 0$, and the variance obtained from the ssLNA accurately estimates the variance of the LNA as $\varepsilon \rightarrow 0$. This example showcases the fact that even though the perturbed equations (62) do not *technically*¹⁰ constitute a singularly perturbed problem in standard form, the ssLNA is capable of generating a highly accurate approximation to the variance; see FIG. 4.

Remark 3. *One should be aware of the fact that the c-nullcline is nearly invariant for sufficiently small e_0 , even if k_3 is comparatively large. However, the limit of only small e_0 ,*

$$\dot{s} = -k_1(\varepsilon e_0 - c)s + k_{-1}c + k_3(s_0 - s - c), \quad (71a)$$

$$\dot{c} = k_1(\varepsilon e_0 - c)s - k_{-1}c - k_2c. \quad (71b)$$

defines a regular perturbation, not a singular perturbation: this is because while the s-axis is invariant when $e_0 = 0$, it contains only a single isolated equilibrium point. The parameter value

$$\hat{\pi} := (k_1, k_2, 0, k_{-1}, k_3, s_0)^T.$$

is a quasi-steady-state parameter value (QSSPV). See [36] and [23] for detailed discussions concerning the difference between TFPVs and QSSPVs.

5. The heuristic reduction of the CME: intimations from the ssLNA

In this section, we discuss the implications that result from our analysis of the reduction of the LNA. Again for simplicity, and because we have chosen to work in arbitrary units, we set $\Omega = 1$.

5.1. Non-elementary propensity functions: standard versus non-standard form

A significant body of literature is dedicated to the analysis of heuristic reductions of CMEs that rely on non-elementary propensity functions. Perhaps the most well-studied example is the Michaelis-Menten reaction mechanism



The CME corresponding to (72) is

$$\frac{\partial}{\partial t} P(n_S, n_C, t) = \left[k_1(E_S^{+1} E_C^{-1} n_S (n_E^T - n_C) + k_{-1}(E_S^{-1} E_C^{+1} - 1)n_C + k_2(E_C^{-1} - 1)n_C \right] P(n_S, n_C, t), \quad (73)$$

¹⁰The word “technically” is emphasized here because earlier analyses [35, 21, 20] indicate there is a sort of standard form behavior near the singular limit.

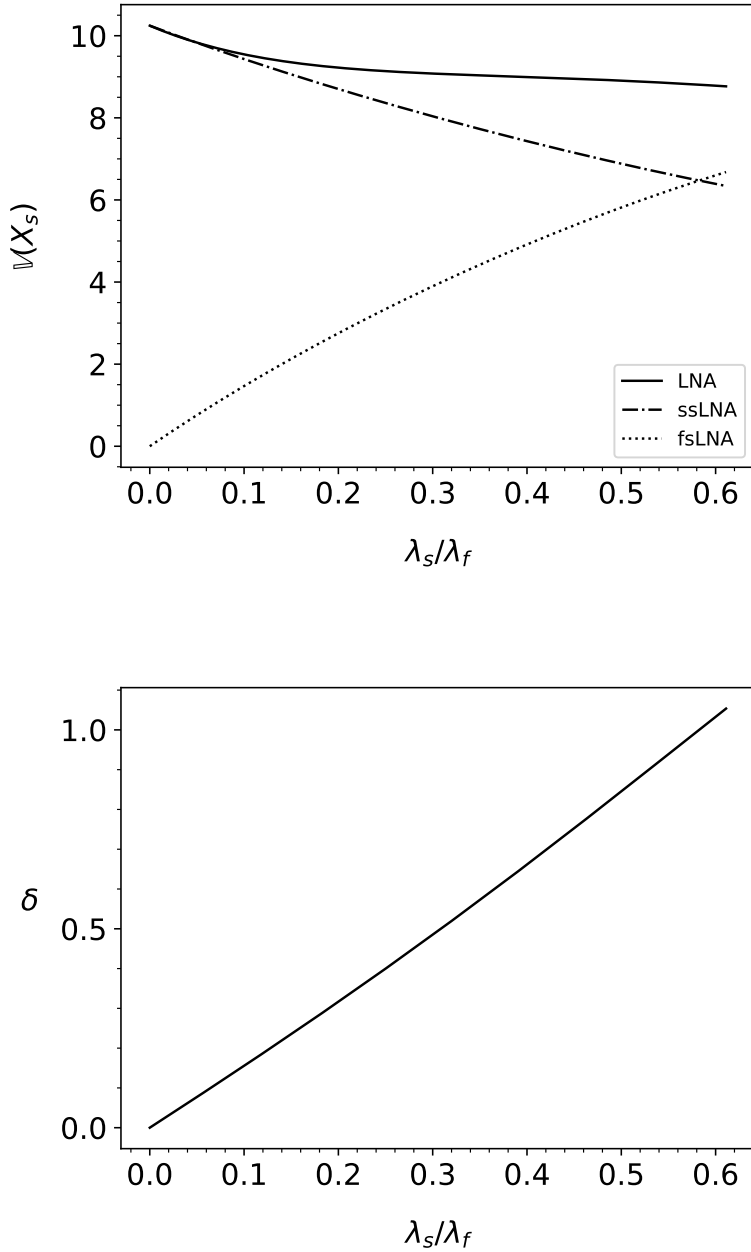


Figure 4: **The ssLNA accurately approximates $\mathbb{V}(X_s)$ in the limit of small e_0 despite not being in standard form.** TOP panel: The variances of X_s obtained from the LNA, the ssLNA, and fs LNA. Note that $\mathbb{V}(X_s)$ from the ssLNA becomes highly accurate as $\lambda_s/\lambda_f \rightarrow 0$. BOTTOM panel: δ versus ε : observe that $\delta \rightarrow 0$ as $\varepsilon \rightarrow 0$. All calculations were computed with the following parameter values (in arbitrary units): $k_1 = 2.0, s_0 = 50.0, k_{-1} = 20.0$; $e_0 = k_3 = \varepsilon$ and ε is varied from 50 to 10^{-3} . By inspection, we see that the difference between $\mathbb{V}(X_s)$ obtained from the ssLNA and the LNA increases with increasing δ .

where n_S denotes the number of substrate molecules, n_C the number of complex molecules, n_E^T is the total number of enzyme molecules, k_1, k_{-1} and k_2 are stochastic rate constants, and

$P(n_S, n_C, t)$ is the probability that the system has n_S substrate molecules and n_C complex molecules at time t .¹¹

The corresponding h CME is

$$\frac{\partial}{\partial t}P(n_S, t) = (E_S^{+1} - 1) \frac{k_2 n_E^T n_S}{K_M + n_S} P(n_S, t), \quad (74)$$

which utilizes the non-elementary propensity function

$$P(n_S - 1, t + dt | n_S, t) := a(n_S)dt = \frac{k_2 n_E^T n_S}{K_M + n_S} dt. \quad (75)$$

Thus, from a purely computational point of view, realizations of the h CME are obtained by supplying the Gillespie algorithm with the non-elementary propensity function (75). Note that (75) has been adapted directly from—and is the stochastic analogue to—the deterministic reduction for substrate concentration, s ,

$$\dot{s} = -\frac{k_2 e_0 s}{K_M + s} \quad (76)$$

which is known as the standard quasi-steady-state approximation (sQSSA) [20, 21, 35]. The utility of (74) lies in the fact that one does not have to simulate the fast binding and unbinding of substrate and enzyme to form complex; (74) accurately estimates the mean and variances of n_S over the time course of the reaction whenever e_0 is sufficiently small. Not only is (74) highly accurate, but its accuracy depends on the homologous conditions that ensure the accuracy of the deterministic counterpart (76); see [3, 29, 39] for details.

Methods to determine the a priori accuracy of h CMEs generally rely on the LNA. This is because the LNA can be derived from the CME via a Ω -expansion [37, 38]. Perhaps the most effective strategy for determining the a priori accuracy of the h CME, introduced by Thomas et al. [17], is to compare the variances of the ssLNA with the LNA of the h CME under steady-state conditions. However, one should also be aware that since the accuracy of the ssLNA depends on the choice of coordinates, so too may the accuracy of h CME. For example, let $n_S^{tot.}$ denote the total number of substrate molecules (a conserved quantity) and consider the following h CME for (47) with propensity functions

$$P(n_S + 1, t + dt | n_S, t) := a^+(n_S)dt = \frac{k_3 (n_S + K_S)^2}{n_E^T K_S + (n_S + K_S)^2} \left(n_S^{tot.} - n_S - \frac{n_E^T n_S}{K_S + n_S} \right) dt \quad (77a)$$

$$P(n_S - 1, t + dt | n_S, t) := a^-(n_S)dt = \frac{k_2 n_E^T n_S (n_S + K_S)}{n_E^T K_S + (n_S + K_S)^2} dt, \quad (77b)$$

which are based on (52). From our analysis of the LNA, the ssLNA significantly underestimates the variance under steady-state conditions, and therefore one can hypothesize that the h CME also underestimates the variances when the system size is sufficiently large. Numerical simulations confirm that the h CME for n_S with propensity functions given by (77) fails to estimate the variance under steady-state conditions; see FIG. 5.

¹¹ $E_X^{\pm j}$ are step operators $E_X^{\pm j} f(X, Y, Z) = f(X \pm j, Y, Z)$; see for [37, 38] for details.

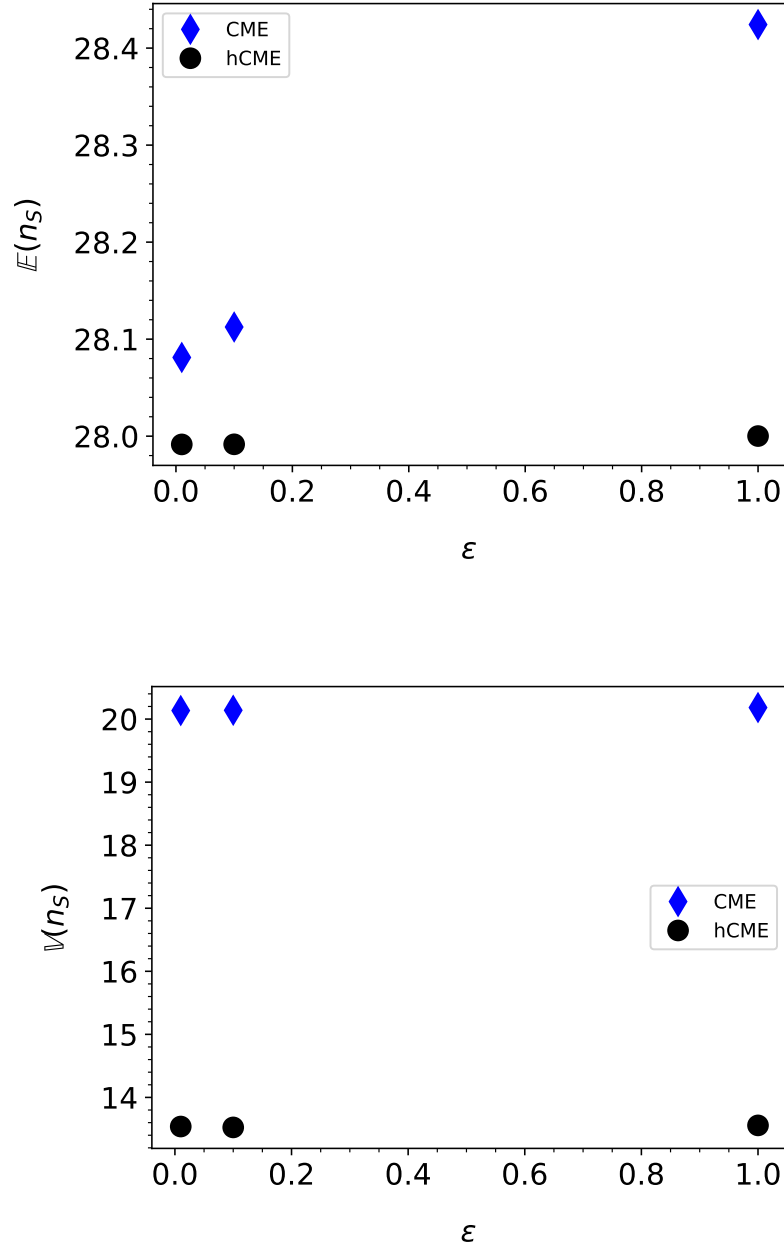


Figure 5: Parameters (arbitrary units): $\Omega = 1.0$, $k_2 = k_3 = \epsilon$, n_E^T , the total number of enzyme molecules = 100, $k_{-1} = 50.0$, and $n_S^{tot.} = 100$. The small rate constants, k_2 and k_3 are equal to ϵ , which varies from 1.0 to 10^{-2} . TOP: The black circles are the numerically-computed substrate means from the Gillespie algorithm applied to the *hCME* (77); the blue diamonds are the numerically-computed substrate means obtained via applying the Gillespie algorithm to the full CME (73). Here we see that the *hCME* accurately approximates the mean. BOTTOM: The black circles are the numerically-computed substrate variances $V(n_S)$ from the *hCME*; the blue diamonds are numerically-computed variances under steady-state conditions obtained from the full CME. In this panel we see that the *hCME* fails to accurately approximate the variance of n_S .

To remedy this problem, we change coordinates and transform the underlying singular perturbation problem into standard form. The *hCME* based on (57) uses the non-elementary propensity functions:

$$P(n_T + 1, t + dt | n_T, t) := a^+(n_T)dt = k_3(n_S^{tot.} - n_T)dt \quad (78a)$$

$$P(n_T - 1, t + dt | n_T, t) := a^-(n_T)dt = \frac{k_2}{2} \left(\gamma - \sqrt{\gamma^2 - 4n_E^T n_T} \right) dt \quad (78b)$$

where n_T is the total number of substrate and complex molecules and

$$\gamma := n_E^T + K_S + n_T.$$

Numerical simulations confirm that the *hCME* accurately estimates the mean and variance of n_T under steady-state conditions when k_2 and k_3 are sufficiently small; see FIG. 6.

Finally, we consider the accuracy of the *hCME* equipped with the propensity functions

$$\begin{aligned} a^+(n_S) &= k_3(n_S^T - n_S), \\ a^-(n_S) &= \frac{k_2 n_E^T n_S}{K_M + n_S}, \end{aligned}$$

which may be valid in the limit of small n_E^T and small k_3 . However, since the corresponding *hLNA*

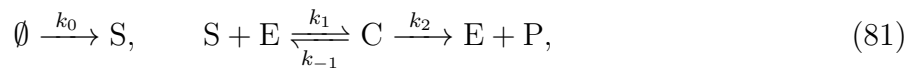
$$dX_s = - \left(\frac{k_2 e_0 K_M}{(K_M + s_{eq.})^2} + k_3 \right) X_s dt + \sqrt{k_3 (s_0 - s_{eq.})} dW_1 - \sqrt{\frac{e_0 s_{eq.}}{K_M + s_{eq.}}} dW_2 \quad (80)$$

does not agree with the *ssLNA* (see FIG. 7), it is unlikely that the *hCME* (79) will prevail under steady-state conditions, and this was confirmed in an earlier work by Agarwal et al. [15]. This example illustrates that the accuracy of the *ssLNA* does not imply the accuracy of the *hLNA*.

On the other hand, numerical evidence strongly suggests that increasing s_0 as well as the steady-state concentration of s dramatically improves the performance of the *hLNA*; see FIG. 8. Moreover, numerical evidence also suggests that increasing k_{-1} so that $k_2 \ll k_{-1}$ also improves the accuracy of the *hLNA*. This may appear to be rather mysterious, but we will show in Section 6 that this kind of improvement is to be expected under these circumstances.

6. The *open* Michaelis-Menten reaction mechanism and the *ssLNA*

We next consider a simple reaction whose analysis is unexpectedly complicated [36]. The open Michaelis-Menten reaction mechanism



is the MM reaction mechanism supplied with a constant influx of substrate [36, 17, 40]. In the limit of small k_0 and small e_0 , the deterministic mass action equations are

$$\dot{s} = \varepsilon k_0 - k_1(\varepsilon e_0 - c)s + k_{-1}c, \quad (82a)$$

$$\dot{c} = k_1(\varepsilon e_0 - c)s - (k_{-1} + k_2)c. \quad (82b)$$

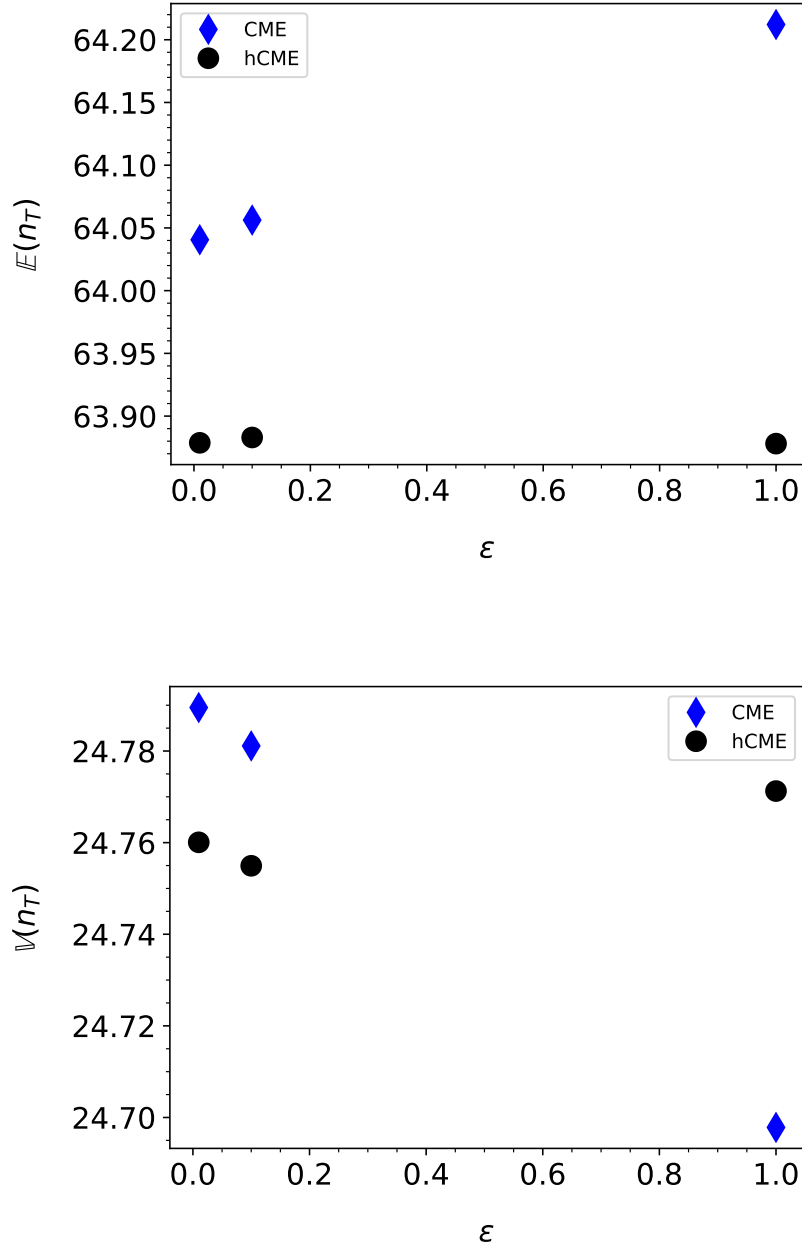


Figure 6: Parameters (arbitrary units): $\Omega = 1.0$, $k_2 = k_3 = \varepsilon$, n_E^T , the total number of enzyme molecules = 100, $k_{-1} = 50.0$, and $n_S^{tot.} = 100$. The small rate constants, k_2 and k_3 are equal to ε , which varies from 1.0 to 10^{-2} . TOP: The black circles are the numerically-computed total substrate means from the *hCME* (78); the blue diamonds are the numerically-computed substrate averages obtained from the full CME. Here we see that the *hCME* accurately approximates the mean. BOTTOM: The black circles are the numerically-computed total substrate variances obtained from Gillespie algorithm applied to the *hCME*; the blue diamonds are the numerically-computed variances obtained from the Gillespie algorithm applied to the full CME. In this panel we see that the *hCME* accurately approximates the variance of n_T .

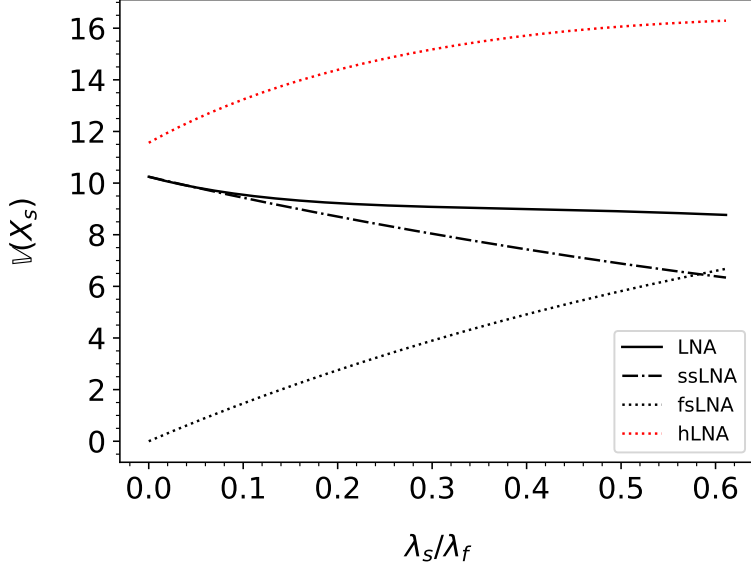


Figure 7: **The ssLNA accurately approximates $\mathbb{V}(X_s)$ in the limit of small e_0 despite not being in standard form; however, the hLNA does not accurately estimate the LNA.** The variances of X_s obtained from the LNA, the ssLNA, the fsLNA, and the hLNA (79). Note that $\mathbb{V}(X_s)$ from the ssLNA (69) does not converge to $\mathbb{V}(X_s)$ from (79) as the eigenvalue ratio goes to zero. All calculations were computed with the following parameter values (in arbitrary units): $k_1 = 2.0, s_0 = 50.0, k_{-1} = 20.0; e_0 = k_3 = \varepsilon$ and ε is varied from 50 to 10^{-3} .

The system (82) has a stationary point located in the first quadrant if $k_0 < k_2 e_0$, and therefore we set $k_0 = \alpha k_2 e_0$ for $\alpha \in [0, 1)$. The steady-state concentration (expressed in terms of α) is

$$\tilde{s} = \frac{\alpha K_M}{1 - \alpha}, \quad \tilde{c} = \alpha e_0, \quad (83)$$

and the corresponding reduced equation is

$$s' = k_0 - \frac{k_2 e_0 s}{K_M + s}. \quad (84)$$

Remark 4. *The reduced equation*

$$\dot{s} = k_0 - \frac{k_2 \varepsilon e_0 s}{K_M + s} \quad (85)$$

is valid for small e_0 . However, the perturbed problem

$$\dot{s} = k_0 - k_1(\varepsilon e_0 - c)s + k_{-1}c, \quad (86a)$$

$$\dot{c} = k_1(\varepsilon e_0 - c)s - (k_{-1} + k_2)c. \quad (86b)$$

is a regular perturbation, not a singular perturbation. A singular perturbation requires small k_0 in addition to small e_0 . Thus,

$$\pi^* := (0, k_1, k_2, k_{-1}, 0, s_0)^T.$$

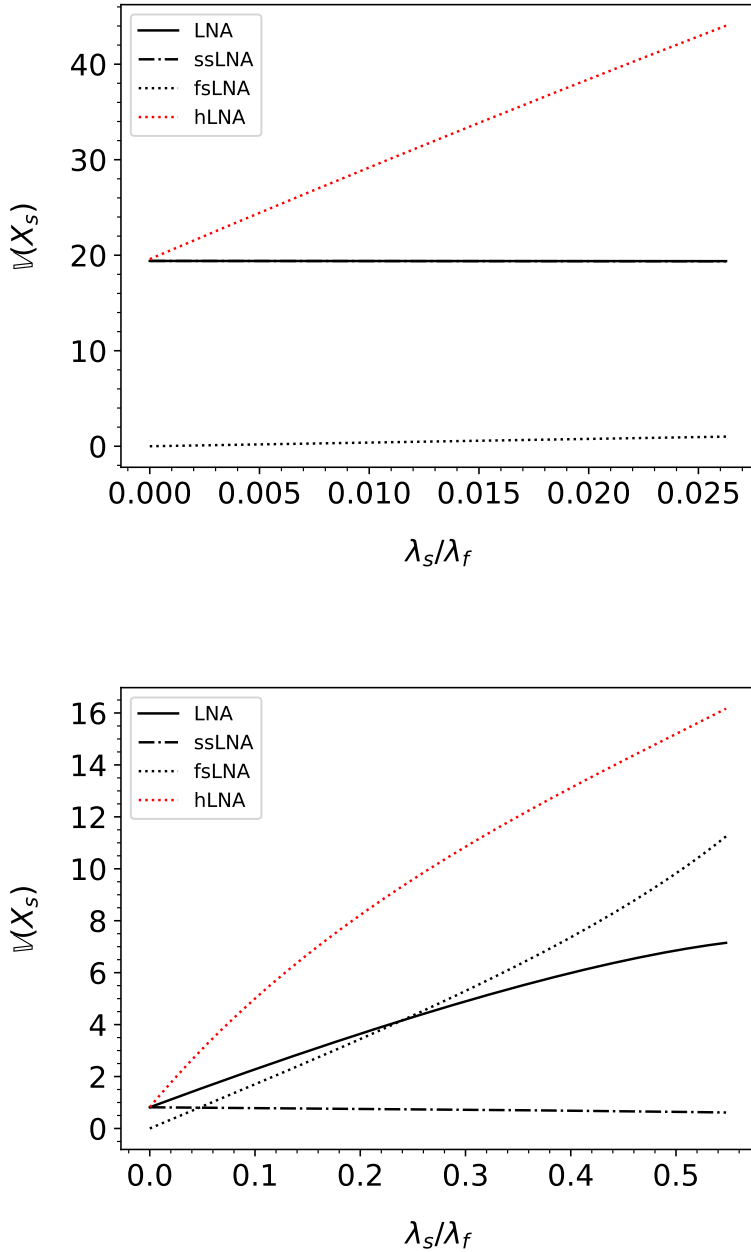


Figure 8: **The ssLNA, hLNA, and the LNA all agree when $e_0 \ll K_M$ and $K_M \ll s_0$ or when $e_0 \ll K_M$ and $k_2 \ll k_{-1}$.** The variances of X_s obtained from the LNA, the ssLNA, the fsLNA, and the hLNA (79). TOP: All calculations where computed with the following parameter values (in arbitrary units): $k_1 = 2.0, s_0 = 1000.0, k_{-1} = k_2 = 20.0$; $e_0 = k_3 = \varepsilon$ and ε is varied from 50 to 10^{-3} . BOTTOM: All calculations where computed with the following parameter values (in arbitrary units): $k_1 = 2.0, s_0 = 1000.0, k_{-1} = 20.0, k_2 = 1.0$; $e_0 = k_3 = \varepsilon$ and ε is varied from 50 to 10^{-3} .

is a TFPV, and the parameter value

$$\hat{\pi} := (k_0, k_1, k_2, k_{-1}, 0, s_0)^T.$$

is a QSSPV.

From the deterministic analysis, we expect the h CME equipped with propensity functions

$$\begin{aligned} a^+(n_S) &= k_0, \\ a^-(n_S) &= \frac{k_2 n_E^T n_S}{K_M + n_S}, \end{aligned}$$

to accurately approximate the mean and standard deviation of n_S under steady-state conditions when e_0 is sufficiently small. Unfortunately, this is not necessarily the case. A careful investigation by Thomas et al. [17] reveals that the variance of LNA obtained from the h CME approximates the variance of the full LNA if and only if $e_0 \ll K_M + \tilde{s}$ and

$$\frac{\beta\alpha(1-\alpha)}{1+\beta(1-\alpha(1-\alpha))} \ll 1, \quad \beta = k_2/k_{-1}. \quad (88)$$

Thus, small enzyme concentration alone is not enough to ensure the validity of the h CME. The question then becomes, how do we interpret the additional constraint (88)?

Consider the mass action equations with the initial conditions $(s_T, c)(0) = (\tilde{s}, 0)$:

$$\begin{aligned} \dot{s}_T &= k_0, \\ \dot{c} &= k_1 e_0 \tilde{s}. \end{aligned}$$

If s_T is the slow variable, then one would expect

$$\left. \frac{ds_T}{dc} \right|_{(s_T=\tilde{s}, c=0)} = \frac{k_0}{k_1 e_0 \tilde{s}} = \frac{k_2}{k_{-1} + k_2} \cdot (1-\alpha) \ll 1 \equiv \beta(1-\alpha) \ll 1. \quad (90)$$

Furthermore, since $0 \leq c \leq e_0$, we must consider the other extreme with the initial condition $(s_T, c)(0) = (\tilde{s} + e_0, e_0)$. In this case we obtain

$$\left. \frac{ds_T}{dc} \right|_{(s=\tilde{s}, c=e_0)} = -\frac{k_0 - k_2 e_0}{(k_{-1} + k_2) e_0} = \frac{k_2}{k_{-1} + k_2} \cdot (1-\alpha) \ll 1 \equiv \beta(1-\alpha) \ll 1. \quad (91)$$

Remark 5. *The qualifier, $(1-\alpha)\beta \ll 1$ profiles a region in parameter space where the total substrate is conserved in the approach toward the slow manifold. Each individual qualifier, $(1-\alpha) \ll 1$ and $\beta \ll 1$, defines a specific singular perturbation scenario that is of standard form in (s_T, c) coordinates.*

As $\alpha \rightarrow 1$ the steady-state concentration of \tilde{s} is far greater than K_M . In a certain sense, this actually corresponds to a different but related singular perturbation scenario: the reverse quasi-steady-state approximation, which is valid in the limit of small k_0 and small k_{-1} and small k_2 . The remaining qualifier present in (88), $\beta \ll 1$, corresponds to small k_2 and small k_0 . Both scenarios are singular perturbations in standard form in (s_T, c) coordinates. We present their corresponding ssLNAs under steady-state conditions in the subsections that follow. These scenarios also highlight the favorability of the standard form in the reduction of both the LNA and the CME.

6.0.1. *The reverse quasi-steady-state approximation (rQSSA): $\alpha \approx 1$*

In (s_T, c) coordinates, the rQSSA corresponds to small k_0, k_{-1} and k_2 :

$$\dot{s}_T = \varepsilon k_0 - \varepsilon k_2 c \quad (92a)$$

$$\dot{c} = k_1(e_0 - c)(s_T - c) - \varepsilon(k_{-1} + k_2)c. \quad (92b)$$

Under steady-state conditions, the perturbation form of the LNA is

$$\begin{aligned} \begin{pmatrix} dX_T \\ dX_c \end{pmatrix} &= \begin{pmatrix} 0 & 0 \\ k_1(e_0 - \tilde{c}) & -k_1(\tilde{s}_T + e_0) + 2k_1\tilde{c} \end{pmatrix} \begin{pmatrix} X_T \\ X_c \end{pmatrix} dt \\ &\quad - \varepsilon \begin{pmatrix} 0 & k_2 \\ 0 & k_{-1} + k_2 \end{pmatrix} \begin{pmatrix} X_T \\ X_c \end{pmatrix} dt + GdW. \end{aligned} \quad (93)$$

The critical manifold is

$$S_0 := \{(X_T, X_c) \in \mathbb{R}^2 : k_1(e_0 - \tilde{c})X_T - k_1(\tilde{s}_T + e_0)X_c + 2k_1\tilde{c}X_c = 0\}, \quad (94)$$

and the ssLNA is

$$dX_T = -\frac{k_2(e_0 - \tilde{c})X_T}{(\tilde{s}_T + e_0 - 2\tilde{c})} dt + \sqrt{k_0} dW_1 - \sqrt{\frac{k_2 e_0 \tilde{s}}{K_M + \tilde{s}}} dW_4, \quad (95a)$$

$$\sim -\frac{k_2 e_0 K_M X_T}{\tilde{s}_T^2} dt + \sqrt{k_0} dW_1 - \sqrt{\frac{k_2 e_0 \tilde{s}}{K_M + \tilde{s}}} dW_4, \quad (95b)$$

as both $e_0/\tilde{s} \rightarrow 0$ and $K_M/\tilde{s} \rightarrow 0$. The hCME for s has the following LNA:

$$dX_s = -\frac{k_2 e_0 K_M X_s}{(\tilde{s} + K_M)^2} dt + \sqrt{k_0} dW_1 - \sqrt{\frac{k_2 e_0 \tilde{s}}{K_M + \tilde{s}}} dW_4, \quad (96a)$$

$$\sim -\frac{k_2 e_0 K_M X_s}{\tilde{s}^2} dt + \sqrt{k_0} dW_1 - \sqrt{\frac{k_2 e_0 \tilde{s}}{K_M + \tilde{s}}} dW_4. \quad (96b)$$

Remark 6. *If $e_0 \ll \tilde{s}$, then $\tilde{s}_T \sim \tilde{s}$, and the total substrate concentration is approximately equal to the substrate concentration since the complex concentration is negligible in comparison to the substrate concentration.*

Thus, we see that two LNAs become indistinguishable as long as $e_0 \ll \tilde{s}$ and $K_M \ll \tilde{s}$. However, the influx rate k_0 must be sufficiently large for $K_M \ll \tilde{s}$ and thus it is necessary that $\alpha \rightarrow 1$. Collectively, these qualifiers imply

$$e_0 \ll K_M + \tilde{s} \quad \text{and} \quad 1 - \alpha \ll 1,$$

which also corresponds to a singular perturbation scenario in standard form.

6.0.2. *Slow product formation and substrate influx: $\beta \ll 1$*

The vector

$$\pi^* := (0, k_1, 0, k_{-1}, e_0, s_0)^T,$$

is a TFPV and the scaled mass action equations for small k_2 and k_0 are

$$\dot{s}_T = \varepsilon k_0 - \varepsilon k_2 c \tag{97a}$$

$$\dot{c} = k_1(e_0 - c)(s_T - c) - k_{-1}c - \varepsilon k_2 c. \tag{97b}$$

By inspection, the critical manifold is

$$S_0 := \{(s_T, c) \in \mathbb{R}^2 : k_1(e_0 - c)(s_T - c) - k_{-1}c = 0\}.$$

The associated LNA is, under steady-state conditions is

$$\begin{aligned} \begin{pmatrix} dX_T \\ dX_c \end{pmatrix} &= \begin{pmatrix} 0 & 0 \\ k_1(e_0 - \tilde{c}) & -k_1(\tilde{s}_T + e_0 + K_S) + 2k_1\tilde{c} \end{pmatrix} \begin{pmatrix} X_T \\ X_c \end{pmatrix} dt \\ &\quad - \varepsilon \begin{pmatrix} 0 & k_2 \\ 0 & k_2 \end{pmatrix} \begin{pmatrix} X_T \\ X_c \end{pmatrix} dt + GdW. \end{aligned} \tag{98}$$

Taking the singular and thermodynamic limits defines the the critical manifold

$$S_0 := \{(X_T, X_c) \in \mathbb{R}^2 : k_1(e_0 - \tilde{c})X_T - k_1(\tilde{s}_T + e_0 + K_S)X_c + 2k_1\tilde{c}X_c = 0\},$$

for which the corresponding ssLNA is

$$dX_T = -\frac{k_2(e_0 - \tilde{c})X_T}{(\tilde{s}_T + e_0 + K_S - 2\tilde{c})} dt + \sqrt{k_0} dW_1 - \sqrt{\frac{k_2 e_0 \tilde{s}}{K_M + \tilde{s}}} dW_4. \tag{99}$$

Next, if $e_0 \ll K_S + \tilde{s}$, then $s_T \sim s$ and

$$dX_T \sim -\frac{k_2 K_M e_0 X_T}{(\tilde{s}_T + K_S)(\tilde{s}_T + K_M)} dt + \sqrt{k_0} dW_1 - \sqrt{\frac{k_2 e_0 \tilde{s}}{K_M + \tilde{s}}} dW_4, \tag{100}$$

which is virtually identical to (96) when $\beta \ll 1$. Thus, we see once again that the qualifiers

$$e_0 \ll K_M + \tilde{s} \quad \text{and} \quad \beta \ll 1,$$

correspond to a special case of a standard form singular perturbation.

6.0.3. *Rapid product formation and slow substrate influx*

As a final example, we consider the TFPV

$$\pi^* := (0, 0, k_2, 0, e_0, s_0)^T,$$

which defines a singular perturbation in (s, c) coordinates

$$\dot{s} = \varepsilon k_0 - \varepsilon k_1(e_0 - c)s + \varepsilon k_{-1}c,$$

$$\dot{c} = \varepsilon k_1(e_0 - c)s - \varepsilon k_{-1}c - k_2 c.$$

The *linear* reduced equation is

$$s' = k_0 - k_1 e_0 s. \quad (102)$$

The ssLNA under steady-state conditions is

$$dX_s = -k_1 e_0 X_s + \sqrt{k_0} dW_1 - \sqrt{k_1 e_0 \tilde{s}} dW_2. \quad (103)$$

Again, if we compare (103) to the *hLNA*

$$dX_s = -\frac{k_2 e_0 K_M X_s}{(\tilde{s} + K_M)^2} dt + \sqrt{k_0} dW_1 - \sqrt{\frac{k_2 e_0 \tilde{s}}{K_M + \tilde{s}}} dW_4, \quad (104)$$

we see that (104) is identical to (103) in the limit of large k_2 . However, there is a caveat: since the reduced equation is linear, it is only valid near the origin $(s, c) = 0$. The steady-state concentration will be close to the origin if $k_0 \ll k_2 e_0$, which implies that $\alpha \ll 1$. Moreover, if $\alpha \ll 1$ then $\tilde{s} \ll K_M$. In this case

$$dX_s \sim -\frac{k_1 k_2 e_0 X_s}{(k_{-1} + k_2)} dt + \sqrt{k_0} dW_1 - \sqrt{\frac{k_1 k_2 e_0 \tilde{s}}{k_{-1} + k_2}} dW_4, \quad (105)$$

which is approximately equal to (103) when $k_{-1} \ll k_2$.

It is worth noting that Kim et al. [41] suggested

$$\frac{\tilde{s} + K_S}{\tilde{s} + K_M} \ll 1 \quad (106)$$

as an additional qualifier¹² for the validity of the *hCME* in their analysis of (47). This is correct, since demanding that (106) holds essentially forces the parameters into a region (i.e., large k_2) where the underlying singularly perturbed is of standard form in (s, c) coordinates.

We conclude this section by noting that our analysis of the open MM reaction also explains the improved performance of the *hLNA* reported in FIG. 8.

7. Discussion

From our analysis presented in Sections 3-6, we can hypothesize that the accuracy of an *hCME* will be fairly good when the underlying singular perturbation problem is

1. Expressed in the standard form with distinct slow and fast variables.
2. Is equipped with a normally hyperbolic and attracting critical manifold.

It is however important to emphasize that neither of these conditions are necessary in order to derive highly accurate reductions in the deterministic regime. For example, consider the reaction offered by Janssen as a counterexample:



¹²In addition to the usual qualifier, namely that $e_0 \ll K_M + \tilde{s}$.

Janssen [13] considered the scaling $k_1 \mapsto \varepsilon^2 k_1, k_2 \mapsto \varepsilon k_2$, which yields the following singular perturbation problem:

$$\dot{x} = -\varepsilon^2 k_1 x + \varepsilon k_2 y, \quad (108a)$$

$$\dot{y} = \varepsilon^2 k_1 x - \varepsilon k_2 y - 2k_3 y^2. \quad (108b)$$

The critical manifold is given by $y = 0$, but the Jacobian of the layer problem is identically zero at any point belonging to the critical manifold. Thus, there is no eigenvalue disparity in the singular limit: both eigenvalues vanish and therefore the critical manifold fails to be normally hyperbolic. Furthermore, we find ourselves at a bit of an impasse: Since the Jacobian is identically zero along S_0 , the usual reduction method – center manifold theory – is not useful, and it is unclear how to rigorously construct a reduced equation that is valid on slow timescales. Of course, one could attempt to construct an asymptotic approximation to the invariance equation, but convergence is not guaranteed. Moreover, an asymptotic solution to the invariance equation does not lead to a detailed portrait of the phase-plane dynamics, which is important as there are clearly processes that unfold on timescales of order 1, ε and ε^2 .

The loss of normal hyperbolicity does not prevent the rigorous construction of a reduced equation. A cylindrical blow-up¹³ of the critical manifold justifies the reduction utilized by Janssen [13]; see Appendix for details. However, as we stated earlier, heuristic reduction in the stochastic regime may be far more sensitive to eigenvalue disparity, and is perhaps more favorable when 1 and 2 hold. Janssen formulated an approximation to the reduced flow of (108) using a rescaling strategy (again, we provide justification for this in the Appendix) and demonstrated with great clarity that stochastic quasi-steady-state approximation based on his reduction of (108) fails.

To examine our hypothesis, we look for a singular perturbation scenario that is equipped with a normally hyperbolic critical manifold in the singular limit and admits a tractable transformation to standard form. Note that the scaling

$$\dot{x} = -\varepsilon k_1 x + \varepsilon k_2 y, \quad (109a)$$

$$\dot{y} = \varepsilon k_1 x - \varepsilon k_2 y - 2k_3 y^2, \quad (109b)$$

is also problematic since we are left with the same difficulty encountered in the singular limit of (108). Instead, consider the scaling $k_3 \mapsto \varepsilon k_3$:

$$\dot{x} = -k_1 x + k_2 y, \quad (110a)$$

$$\dot{y} = k_1 x - k_2 y - 2\varepsilon k_3 y^2. \quad (110b)$$

From the layer problem, we see that $x + y$ is conserved, which implies z is also conserved. Using the stoichiometric relationship $x + y + 2z = x(0) + y(0) + 2z(0) = \alpha$ permits us to write down the standard form

$$\dot{y} = k_1(\alpha - y - 2z) - k_2 y - 2\varepsilon k_3^2, \quad (111a)$$

$$\dot{z} = \varepsilon k_3 y^2. \quad (111b)$$

¹³For details concerning the blow-up method in the context of singular perturbations, we refer the reader to Krupa and Szmolyan [26], as well as Kuehn [25] and Wechselberger [7].

The reduced equation that follows is

$$z' = \frac{k_3 k_1^2}{(k_1 + k_2)^2} \cdot (\alpha - 2z)^2. \quad (112)$$

Converting (112) into a stochastic propensity function yields excellent results when α is even, which further supports our hypothesis; see FIG. 9.

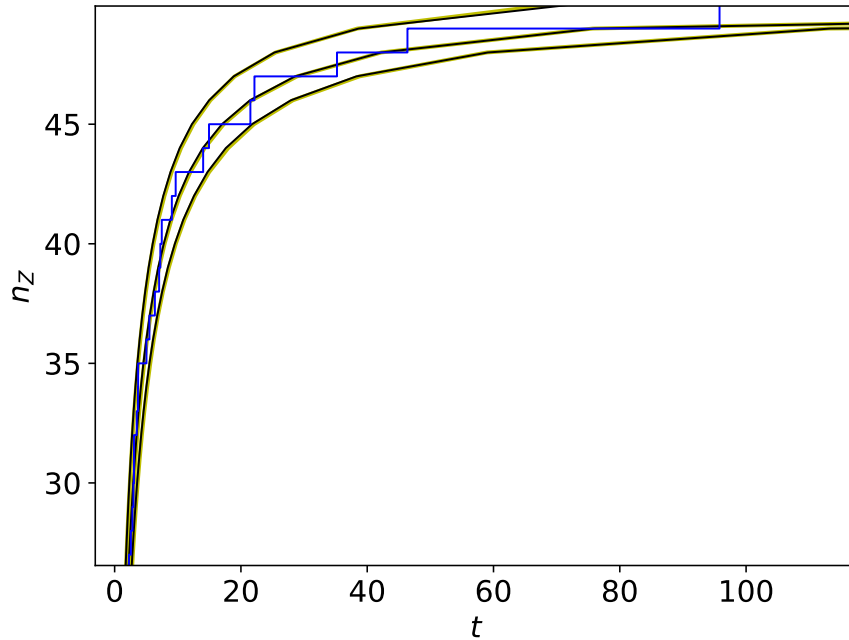


Figure 9: **Stochastic propensity functions adapted from standard form deterministic models are favorable.** The yellow curves are the mean and mean \pm one standard deviation obtained from the 10000 realizations of the Gillespie algorithm. The black line are the mean and mean \pm one standard deviation obtained from the modified Gillespie algorithm with a single propensity function adapted from (112). The blue line is a single realization. Clearly, the *h*CME accurately approximates the full CME over the complete time course of the reaction. Parameters (in arbitrary units): $k_1 = 10, k_2 = 10, k_3 = 0.01, n_X = 50, n_Y = 50$ and $\Omega = 1.0$.

Our analysis reveals that the reduction of stochastic models (based on heuristics) is sensitive to the choice of coordinate system in addition to eigenvalue disparity. This is markedly different from the deterministic case where Fenichel theory provides a coordinate-free framework for computing accurate reduced equations irregardless of whether or not the system is in standard form. Moreover, the blow-up method provides a means of extending Fenichel theory to scenarios where eigenvalue disparity is nonexistent in the singular limit. In the LNA regime it is possible to compute a reduced equation for cases without eigenvalue disparity in the singular limit via Ω -expansion; again, see [13] for details. However, the reduction of the CME in such cases appears to be an open problem that warrants additional research.

8. Appendix

To determine a reduced equation for that is valid for $0 < \varepsilon \ll 1$ we blow-up¹⁴ the critical manifold,

$$S_0 := \{(x, y) \in \mathbb{R}^2 : y = 0\}.$$

To begin, we append $\dot{\varepsilon} = 0$ to the mass action equations, and define $F(x, y, \varepsilon) : \mathbb{R}^3 \mapsto T\mathbb{R}^3$:

$$\begin{pmatrix} \dot{x} \\ \dot{y} \\ \dot{\varepsilon} \end{pmatrix} = \begin{pmatrix} -\varepsilon^2 k_1 x + \varepsilon k_2 y \\ \varepsilon^2 k_1 x - \varepsilon k_2 y - 2k_3 y^2 \\ 0 \end{pmatrix} =: F(x, y, \varepsilon). \quad (113)$$

The objective is to rewrite (113) in terms of *generalized* polar coordinates of the form

$$x = \bar{r}^{\gamma_1} \bar{x}, \quad y = \bar{r}^{\gamma_2} \bar{y}, \quad \varepsilon = \bar{r}^{\gamma_3} \bar{\varepsilon}, \quad (114)$$

where $(\gamma_1, \gamma_2, \gamma_3) \in \mathbb{N}^3$, $(\bar{x}, \bar{y}, \bar{\varepsilon}) \in \mathbb{S}^2$, and $\bar{r} \in [0, \rho] := I$. Since our interest is in the behavior of the system when ε and y are small we choose $\gamma_1 = 0$ and $\bar{s} = s$. The additional weights γ_2, γ_3 are determinable from the quasi-homogeneity (or homogeneity) of the vector field. For our purposes, $\gamma_2 = \gamma_3 = 1$ will suffice. The blow-up variables $(\bar{y}, \bar{\varepsilon}, \bar{r})$ satisfy

$$(\bar{y}, \bar{\varepsilon}) \in \mathbb{S}^1 : \bar{y}^2 + \bar{\varepsilon}^2 = 1, \quad \bar{r} \in [0, \rho] := I. \quad (115)$$

Thus, we define the map $\varphi : \mathbb{S}^1 \times I \mapsto \mathbb{R}^2$:

$$\varphi(\bar{y}, \bar{\varepsilon}, \bar{r}) = (\bar{r}\bar{c}, \bar{r}\bar{\varepsilon}) \quad (116)$$

or, including x , we have $\widehat{\varphi}(x, \bar{y}, \bar{\varepsilon}, \bar{r}) : \mathbb{R} \times \mathbb{S}^2 \times I \mapsto \mathbb{R}^3$.

$$\widehat{\varphi}(x, \bar{c}, \bar{\varepsilon}, \bar{r}) = (x, \bar{r}\bar{c}, \bar{r}\bar{\varepsilon}). \quad (117)$$

The blow-up of $F(x, y, \varepsilon)$, which we denote as $\widehat{F}(x, \bar{y}, \bar{\varepsilon}, \bar{r})$, is formally given by

$$\widehat{F}(x, \bar{y}, \bar{\varepsilon}, \bar{r}) := (D\widehat{\varphi}^{-1} \circ F \circ \widehat{\varphi})(x, \bar{y}, \bar{\varepsilon}, \bar{r}), \quad (118)$$

which is defined for $0 < \bar{r}$ and extends continuously to $\bar{r} = 0$. The objective is then to analyze the dynamics in a neighborhood of $\bar{r} = 0$. While \widehat{F} and F are diffeomorphic for $\bar{r} \neq 0$, it does not appear – at first glance – that the difficulty arising from the degenerate critical manifold has a clear resolution since the flow of the extension of $\widehat{F}(x, \bar{y}, \bar{\varepsilon}, \bar{r})$ to $\bar{r} = 0$ is trivial. However, rescaling by \bar{r} does not destroy (in the topological sense) the qualitative landscape of the phase portrait for $0 < \bar{r}$

$$\bar{F}(x, \bar{y}, \bar{\varepsilon}, \bar{r}) = \frac{1}{\bar{r}} \cdot \widehat{F}(x, \bar{y}, \bar{\varepsilon}, \bar{r}). \quad (119)$$

Therefore, orbits of $\bar{F}(x, \bar{y}, \bar{\varepsilon}, \bar{r})$ correspond to the orbits of $F(x, y, \varepsilon)$ for $0 < \bar{r}$. Most important is that both \widehat{F} and \bar{F} are defined (by continuous extension) on $\mathbb{S}^1 \times \{\bar{r} = 0\}$ [44], and

¹⁴The blow-up method was originally developed in the context of isolated nilpotent singularities; see for example [42, 43].

the cylindrical blow-up of the x -axis (i.e., the blow-up of the critical manifold of $F(x, y, 0)$) is

$$\lim_{\bar{r} \rightarrow 0} \frac{1}{\bar{r}} \cdot \widehat{F}(x, \bar{y}, \bar{\varepsilon}, \bar{r}). \quad (120)$$

The power resides in the fact that the flow on the cylinder (120) is non-trivial, and the critical manifold that emerges on (120) is normally hyperbolic. Therefore, classical Fenichel theory applies and highly accurate approximations to the slow dynamics can be computed that are valid for $0 < \bar{r}$.

Remark 7. *This is the remarkable power behind what is essentially a (generalized) polar coordinate transformation: For the case of critical manifolds, Fenichel theory applies to the desingularized flow on the blown-up cylinder that contains a normally hyperbolic critical manifold and it is therefore possible to find a reduced equation that is valid for $0 < \bar{r}$.*

Given that \mathbb{S}^1 is a compact submanifold of \mathbb{R}^2 , it is necessary to cover $\mathbb{S}^1 \times I$ with local coordinate charts, $\kappa_i : \mathbb{S}^1 \times I \mapsto \mathbb{R}^2$. Once local coordinate charts are selected, we define the map, $\mu \circ \kappa_i \mapsto \mathbb{R}^2$.

$$\begin{array}{ccc} & \mathbb{S}^1 \times I & \\ \kappa \swarrow & & \searrow \varphi \\ \mathbb{R}^2 & \xrightarrow{\mu} & \mathbb{R}^2 \end{array} \quad (121)$$

The dynamics in each relevant coordinate chart is analyzed and a global picture is formulated by stitching the local pictures in each coordinate chart together via transition maps.

Obviously there a choice in the selection of κ_i , and some choices are more convenient than others depending on the vector field of interest. For our purposes, we will take

$$\kappa_1(\bar{y}, \bar{\varepsilon}, \bar{r}) = \left(\frac{\bar{y}}{\bar{\varepsilon}^1}, \frac{\bar{r}}{\bar{\varepsilon}^{-1}} \right) := (y_1, r_1) \in \mathbb{R}^2 \quad (122)$$

and more generally:

$$\widehat{\kappa}_1(x, \bar{y}, \bar{\varepsilon}, \bar{r}) = \left(x, \frac{\bar{y}}{\bar{\varepsilon}^1}, \frac{\bar{r}}{\bar{\varepsilon}^{-1}} \right) := (x, y_1, r_1) \in \mathbb{R}^3. \quad (123)$$

It follows from (121) that $\mu_1 \circ \widehat{\kappa}_1 = (x, r_1 y_1, r_1)$.

Note that κ_i only maps open sets of $\mathbb{S}^1 \rightarrow \mathbb{R}$ for $\bar{\varepsilon} \neq 0$. Thus, one additional chart is required to cover the relevant parts of \mathbb{S}^1 . To account for this we define

$$\kappa_2(\bar{y}, \bar{\varepsilon}, \bar{r}) = \left(\frac{\bar{\varepsilon}}{\bar{y}^1}, \frac{\bar{r}}{\bar{y}^{-1}} \right) := (\varepsilon_2, r_2) \in \mathbb{R}^2 \quad (124)$$

and therefore $\widehat{\mu}_2 \circ \widehat{\kappa}_2 = (x, r_2, \varepsilon_2 r_2)$.

Finally, the transition maps between charts are given by:

$$\kappa_{12} : \quad \varepsilon_2 = y_1^{-1}, \quad r_2 = r_1 y_1, \quad (125a)$$

$$\kappa_{21} : \quad y_1 = \varepsilon_2^{-1}, \quad r_1 = \varepsilon_2 r_2. \quad (125b)$$

We now proceed to work out the dynamics in each chart.

8.0.1. Dynamics in κ_1 .

In local coordinates we have

$$\begin{pmatrix} \dot{x} \\ \dot{y}_1 \\ \dot{r}_1 \end{pmatrix} = \begin{pmatrix} -r_1^2 k_1 x + r_1^2 k_2 y_1 \\ r_1 k_1 x - r_1 k_2 y_1 - 2k_3 r_1 y_1^2 \\ 0 \end{pmatrix} =: \widehat{F}(x, y_1, r_1), \quad (126)$$

and thus r_1 is a parameter in κ_1 . By definition we have that $\bar{F}(x, y_1, r_1)$ is given by

$$\begin{pmatrix} x' \\ y_1' \\ r_1' \end{pmatrix} = \begin{pmatrix} -r_1 k_1 x + r_1 k_2 y_1 \\ k_1 x - k_2 y_1 - 2k_3 y_1^2 \\ 0 \end{pmatrix} =: \bar{F}(x, y_1, r_1). \quad (127)$$

where “ $'$ ” denotes differentiation with respect to $\tau_1 =: r_1 t$. The flow on the cylinder, \mathcal{C} , is thus

$$\begin{pmatrix} x' \\ y_1' \end{pmatrix} = \begin{pmatrix} 0 \\ k_1 x - k_2 y_1 - 2k_3 y_1^2 \end{pmatrix}, \quad (128)$$

which is a singular perturbation problem in standard form. The critical manifold is given by

$$S_0 := \left\{ (x, y_1) \in \mathbb{R} \times \mathbb{S}^1 : y_1 = \frac{-k_2 + \sqrt{k_2^2 + 8k_3 k_1 x}}{4k_3} =: \phi(x) \right\}, \quad (129)$$

which is normally hyperbolic. By Fenichel theory, the slow flow for $0 < r_1$ is given by

$$x' = -r_1 k_1 x + r_1 k_2 \phi(x). \quad (130)$$

Remark 8. *At this point it is important to note that in local coordinates we have $(x, y_1, r_1) = (x, y/\varepsilon, \varepsilon)$, which is equivalent to the original rescaling employed by Janssen who defined $y = \varepsilon z$ to derive (130). For this reason, κ_1 is generally referred to as the scaling chart. Furthermore, in the local coordinate chart $r_1 = \varepsilon$, and the slow flow actually evolves on a timescale $\mathcal{O}(\varepsilon^2)$:*

$$x' = -r_1 k_1 x + r_1 k_2 \phi(x) \equiv \frac{dx}{d(\varepsilon^2 t)} = -k_1 x + k_2 \phi(x). \quad (131)$$

8.0.2. Dynamics in κ_2 .

Once again, in local coordinates we have

$$\begin{pmatrix} \dot{x} \\ \dot{r}_2 \\ \dot{\varepsilon}_2 \end{pmatrix} = \begin{pmatrix} -r_2^2 \varepsilon_2 (k_1 \varepsilon_2 x - k_2) \\ r_2^2 (k_1 \varepsilon_2^2 x - k_2 \varepsilon_2 - 2k_3) \\ -\varepsilon_2 r_2 (k_1 \varepsilon_2^2 x - k_2 \varepsilon_2 - 2k_3) \end{pmatrix} =: \widehat{F}(x, r_2, \varepsilon_2) \quad (132)$$

and therefore

$$\begin{pmatrix} x' \\ r_2' \\ \varepsilon_2' \end{pmatrix} = \begin{pmatrix} -r_2 \varepsilon_2 (k_1 \varepsilon_2 x - k_2) \\ r_2 (k_1 \varepsilon_2^2 x - k_2 \varepsilon_2 - 2k_3) \\ -\varepsilon_2 (k_1 \varepsilon_2^2 x - k_2 \varepsilon_2 - 2k_3) \end{pmatrix} =: \bar{F}(x, r_2, \varepsilon_2), \quad (133)$$

where in this context “ $'$ ” denotes differentiation to $\tau_2 = r_2 t$.

On the cylinder, \mathcal{C} , we once again recover a singular perturbation problem:

$$\begin{pmatrix} x' \\ \varepsilon_2' \end{pmatrix} = \begin{pmatrix} 0 \\ -\varepsilon_2(k_1\varepsilon_2^2x - k_2\varepsilon_2 - 2k_3) \end{pmatrix} \quad (134)$$

which has a corresponding critical manifold

$$S_0 := \left\{ (x, \varepsilon_2) \in \mathbb{R} \times \mathbb{S}^1 : x = \frac{k_2\varepsilon_2 + 2k_3}{k_1\varepsilon_2^2}, \varepsilon_2 \neq 0 \right\}, \quad (135)$$

which is identical to (129) given the transition maps (125).

Note that

$$V := \{(x, r_2, \varepsilon_2) \in \mathbb{R} \times \mathbb{S}^1 \times I : \varepsilon_2 = 0\} \quad (136)$$

is a two-dimensional invariant subspace. The Jacobian, $D\bar{F}(x, r_2, \varepsilon_2)$ along $\mathcal{C} \cap V$ is

$$D\bar{F}(x, r_2, \varepsilon_2)|_{\mathcal{C} \cap V} = \begin{pmatrix} 0 & 0 & 0 \\ 0 & -2k_3 & 0 \\ 0 & 0 & 2k_3 \end{pmatrix} \quad (137)$$

and thus the one-dimensional intersection $\mathcal{C} \cap V$ is a critical manifold of saddle type that describes the link between the ultra fast dynamics off of \mathcal{C} with the dynamics on \mathcal{C} . The flow on V away from \mathcal{C} is

$$r_2' = -2k_3r_2. \quad (138)$$

Note that $(x, r_2, \varepsilon_2) = (x, y, \varepsilon/y)$ and therefore (138) describes the ultra fast dynamics of trajectories approaching the cylinder. On the cylinder, they are given by (134). The Jacobian on \mathcal{C} along S_0 has one zero eigenvalue and one negative eigenvalue. Hence S_0 is attracting and the saddle manifold $\mathcal{C} \cap V$ repels flow on \mathcal{C} towards the critical manifold.

References

- [1] W. Stroberg, S. Schnell, On the estimation errors of K_M and v from time-course experiments using the Michaelis–Menten equation, *Biophys. Chem.* 219 (2016) 17–27.
- [2] Y. Cao, D. T. Gillespie, L. R. Petzold, The slow-scale stochastic simulation algorithm, *J. Chem. Phys.* 122 (2005) 014116.
- [3] K. Sanft, D. T. Gillespie, L. R. Petzold, The legitimacy of the stochastic Michaelis–Menten approximation, *IET Syst. Biol.* 5 (2011) 58–69.
- [4] N. Fenichel, Geometric singular perturbation theory for ordinary differential equations, *J. Differ. Equations* 31 (1979) 53–98.
- [5] N. Fenichel, Persistence and smoothness of invariant manifolds for flows, *Indiana Univ. Math. J.* 21 (1971/72) 193–226.
- [6] A. Tikhonov, Systems of differential equations containing small parameters in their derivatives, *Mat. Sb. (N.S.)* 31 (1952) 575–586.

- [7] M. Wechselberger, Geometric Singular Perturbation Theory Beyond the Standard Forms, number 6 in *Frontiers in Applied dynamical systems: Tutorials and Reviews*, Springer, 2020.
- [8] N. Berglund, B. Gentz, *Noise-induced phenomena in slow-fast dynamical systems*, Springer-Verlag London, Ltd., London, 2006.
- [9] T. Turner, S. Schnell, K. Burrage, Stochastic approaches for modelling in vivo reactions, *Computational Biology and Chemistry* 28 (2004) 165–178.
- [10] C. V. Rao, A. P. Arkin, Stochastic chemical kinetics and the quasi-steady-state assumption: Application to the Gillespie algorithm, *J. Chem. Phys.* 118 (2003) 4999–5010.
- [11] S. MacNamara, A. M. Bersani, K. Burrage, R. B. Sidje, Stochastic chemical kinetics and the total quasi-steady-state assumption: Application to the stochastic simulation algorithm and chemical master equation, *The Journal of Chemical Physics* 129 (2008) 095105.
- [12] E. A. Mastny, E. L. Haseltine, J. B. Rawlings, Two classes of quasi-steady-state model reductions for stochastic kinetics, *J. Chem. Phys.* 127 (2007) 094106.
- [13] J. A. M. Janssen, The elimination of fast variables in complex chemical reactions. III. mesoscopic level, *J. Stat. Phys.* 57 (1989) 187–198.
- [14] P. Thomas, A. V. Straube, R. Grima, Communication: Limitations of the stochastic quasi-steady-state approximation in open biochemical reaction networks, *J. Chem. Phys.* 135 (2011) 181103.
- [15] A. Agarwal, R. Adams, G. C. Castellani, H. Z. Shouval, On the precision of quasi steady state assumptions in stochastic dynamics, *The Journal of Chemical Physics* 137 (2012) 044105.
- [16] J. Kim, K. Josić, M. Bennett, The validity of quasi-steady-state approximations in discrete stochastic simulations, *Biophys. J.* 107 (2014) 783 – 793.
- [17] P. Thomas, A. V. Straube, R. Grima, The slow-scale linear noise approximation: an accurate, reduced stochastic description of biochemical networks under timescale separation conditions, *BMC Sys. Biol.* 6 (2012) 39.
- [18] N. Herath, D. Del Vecchio, Reduced linear noise approximation for biochemical reaction networks with time-scale separation: The stochastic tQSSA⁺, *J. Chem. Phys.* 148 (2018) 094108.
- [19] C. D. Pahlajani, P. J. Atzberger, M. Khammash, Stochastic reduction method for biological chemical kinetics using time-scale separation, *J. Theo. Biol.* 272 (2011) 96–112.
- [20] L. A. Segel, On the validity of the steady state assumption of enzyme kinetics, *Bull. Math. Biol.* 50 (1988) 579–593.

- [21] L. A. Segel, M. Slemrod, The quasi-steady-state assumption: A case study in perturbation, *SIAM Rev.* 31 (1989) 446–477.
- [22] A. Goeke, Reduktion und asymptotische reduktion von reaktionsgleichungen, Doctoral Dissertation, RWTH Aachen (2013).
- [23] A. Goeke, S. Walcher, E. Zerz, Classical quasi-steady state reduction – A mathematical characterization, *Physica D* 345 (2017) 11–26.
- [24] A. Goeke, S. Walcher, E. Zerz, Determining “small parameters” for quasi-steady state, *J. Differential Equations* 259 (2015) 1149–1180.
- [25] C. Kuehn, Multiple time scale dynamics, volume 191 of *Applied Mathematical Sciences*, Springer, 2015.
- [26] M. Krupa, P. Szmolyan, Extending slow manifolds near transcritical and pitchfork singularities, *Nonlinearity* 14 (2001) 1473–1491.
- [27] J. Eilertsen, S. Schnell, S. Walcher, Natural parameter conditions for singular perturbations of chemical and biochemical reaction networks, *Bulletin of Mathematical Biology* 85 (2023) 48.
- [28] P. Thomas, R. Grima, A. V. Straube, Rigorous elimination of fast stochastic variables from the linear noise approximation using projection operators, *Phys. Rev. E* 86 (2012) 041110.
- [29] J. Eilertsen, K. Srivastava, S. Schnell, Stochastic enzyme kinetics and the quasi-steady-state reductions: Application of the slow scale linear noise approximation à la fenichel, *Journal of Mathematical Biology* 85 (2022) 3.
- [30] G. S. Katzenberger, Solutions of a stochastic differential equation forced onto a manifold by a large drift, *Ann. Probab.* 19 (1991) 1587–1628.
- [31] T. L. Parsons, T. Rogers, Dimension reduction for stochastic dynamical systems forced onto a manifold by large drift: a constructive approach with examples from theoretical biology, *J. Phys. A Math. Theor.* 50 (2017) 415601.
- [32] J. A. M. Borghans, R. J. De Boer, L. A. Segel, Extending the quasi-steady state approximation by changing variables, *Bull. Math. Biol.* 58 (1996) 43–63.
- [33] J. K. Kim, J. J. Tyson, Misuse of the Michaelis—Menten rate law for protein interaction networks and its remedy, *PLoS Comp. Biol.* 16 (2020) 1–21.
- [34] C. Lax, S. Walcher, Singular perturbations and scaling, *Discrete and Continuous Dynamical Systems - B* 25 (2020) 1–29.
- [35] F. G. Heineken, H. M. Tsuchiya, R. Aris, On the mathematical status of the pseudo-steady hypothesis of biochemical kinetics, *Math. Biosci.* 1 (1967) 95–113.

- [36] J. Eilertsen, M. Roussel, S. Schnell, S. Walcher, On the quasi-steady-state approximation in an open Michaelis–Menten reaction mechanism, *AIMS Math* 6 (2021) 6781–6814.
- [37] N. V. Kampen, Chapter V. The Master Equation, in: *Stochastic Processes in Physics and Chemistry* (3rd Edition), North-Holland Personal Library, Elsevier, Amsterdam, 2007, pp. 96–133.
- [38] N. V. Kampen, Chapter X. The expansion of the Master Equation, in: *Stochastic Processes in Physics and Chemistry* (3rd Edition), North-Holland Personal Library, Elsevier, Amsterdam, 2007, pp. 244–272.
- [39] H.-W. Kang, W. R. KhudaBukhsh, H. Koepl, G. Rempala, Quasi-steady-state approximations derived from the stochastic model of enzyme kinetics, *Bull. Math. Biol.* 81 (2019) 1303–1336.
- [40] I. Stoleriu, F. A. Davidson, J. L. Liu, Quasi-steady state assumptions for non-isolated enzyme-catalysed reactions, *J. Math. Biol.* 48 (2004) 82–104.
- [41] J. K. Kim, K. Josić, M. R. Bennett, The relationship between stochastic and deterministic quasi-steady state approximations, *BMC Syst. Biol.* 9 (2015) 87.
- [42] A. Bruno, *Local methods in nonlinear differential equations*, Springer, Berlin, 1989.
- [43] F. Dumortier, J. Llibre, J. Artés, *Qualitative theory of planar differential systems*, Springer-Verlag Berlin Heidelberg, 2006.
- [44] F. Dumortier, Singularities of vector fields on the plane, *Journal of Differential Equations* 23 (1977) 53–106.